ELSEVIER

Coordination Chemistry Reviews
144 (1995) 461–511

COORDINATION CHEMISTRY REVIEWS

Metallothioneins

Martin J. Stillman

Department of Chemistry, University of Western Ontario, London, Ont. N6A 5B7, Canada

Received 8 March 1995

Contents

Abstract

Metallothioneins are a class of protein characterized by a high cysteine content (up to 30% of the amino acid residues), low molar mass (approx. 6000 for the mammalian protein), and

SSDI 0010-8545(95)01173-0

lack of aromatic amino acid residues. Remarkable metal binding properties have been reported both in vivo and in vitro. Chemical and spectroscopic studies have shown that an unusually wide range of metals bind to metallothionein. The metallated protein has been well characterized from mammalian sources, yeast, fungus, and crustaceans. Key structural properties have been determined for protein isolated from mammals, yeasts, fungus and crustaceans. ^{113}Cd and ^{1}H NMR techniques have been used successfully to characterize the structures in a number of different proteins. Together with X-ray diffraction results, analyses of these NMR data have established that in mammalian Cd_7-MT and Zn_7-MT, the metals are tetrahedrally coordinated in two isolated domains with stoichiometries of M_4S_{11} and M_3S_9. Overall, the most extensively studied proteins contain Cu(I), Ag(I), Co(II), and Hg(II). Optical spectroscopy, and in particular circular dichroism and luminescence, have provided details of a complicated metal binding chemistry whether metals are added directly to the metal free, apometallothionein, or to the zinc containing protein. Three structural motifs have been identified from studies of Cd(II), Zn(II), Hg(II), Cu(I) and Ag(I) binding. For rabbit liver metallothionein, the peptide chain forms metal thiolate clusters with stoichiometries of M_7-S_{20}, M_{12}-S_{20}, and M_{18}-S_{20} depending on which metal binds. The synchrotron-based techniques of XANES and XAFS have provided a wealth of information on the metal–thiolate bond lengths and coordination geometry of the bound metal, that together with structural information from two-dimensional ^{1}H NMR data should allow three-dimensional structures of a range of metallothioneins to determined in the near future.

Keywords: Metallothioneins; Protein; Metal binding; Spectroscopic properties XAFS, Circular dichroism

1. Introduction

Metallothionein[1] occupies a unique place in the catalog of metalloproteins as demonstrated by a primary sequence dominated by a 30% cysteine content, metal binding properties that include all of the Group 11 and 12 metals[2], and a tertiary structure dominated by metal–thiolate clusters that form in the metal binding sites [1–7].

Metallothioneins are characterized by a low molecular mass (6000–7000 daltons for the mammalian protein), the presence of about 30% by number of cysteinyl residues (in the mammalian protein, 20 cysteines out of a total of 61 or 62), and the complete absence of aromatic amino acids in the primary sequence. The capability of binding 7, 12, or even 18 Group 11 and 12 metals (commonly Cd(II), Cu(I), Hg(II), and Zn(II)), in either a single (yeast or fungus) or two (mammalian and crustacean) clustered domains, makes this protein quite remarkable. Together these properties have led to an almost exponential increase in publications describing different properties since the first reports appeared. Metallothionein was first characterized by Vallee and co-workers starting in the late 1950s in studies that have extended through to today [8–11]. A critical feature has been the determination of the exact metal to cysteine ratios in solutions of the protein. The early studies became considerably easier as the atomic absorption spectrometer was developed and went

[1] The term metallothionein covers a range of proteins that we will describe below.

[2] Using the ACS convention for Groups IB and IIB.

into commercial production [12]. Currently, electrospray mass spectrometry offers a new method by which the molar mass of metallothionein, together with its complement of metals, can be determined with precision. Information on the distribution of isoforms and subisoforms is uniquely provided by the mass spectral patterns [13–15]. The precise determination of the stoichiometric ratio between the bound metals and the number of accessible cysteinyl sulfurs (S_{cys}) has played a critical role in our understanding of the chemistry, biochemistry, and physiological chemistry of this exceptional protein. The development of multinuclear ^{113}Cd and high field ^{1}H NMR techniques led to the elucidation of the metal–thiolate cluster structure for cadmium metallothionein in 1980 [16].

Following the initial reports from Vallee's group [8–10], a number of chemical, spectroscopic, and structural studies established the now familiar but still remarkable metal binding chemistry of the metallothioneins. For example, the series of spectroscopic studies by Weser and coworkers demonstrated from titrations of the protein with different metals (including, Cd(II), and Cu(I)) that several different species existed and that these species exhibited individual spectral properties [17]. The NMR and X-ray studies together showed that the three-dimensional structure for mammalian metallothionein contains Cd(II) and Zn(II) in two separate metal–thiolate cluster domains [2,4,6,7,16]. These stoichiometric and structural properties are now identified as key properties for each of the three classes of peptide (which are known as metallothionein classes I, II and III). The formation of the metal–thiolate cluster has been the basis for the interpretation of much subsequent research.

The general structural properties that characterize all metallothioneins are the formation of metal–thiolate clusters that involve terminal and/or bridging cysteinyl thiolate groups of the peptide chain. The tertiary structure of the metallated protein is then completely dominated by the manner in which the peptide chain wraps round these clusters. In the short peptide metallothioneins from yeast and fungus, a single metal binding domain has been proposed [18]. Whereas in the longer peptide chains found for crustacean (with 18 cysteines for crab MT [18] and lobster [18,19]), and for mammalian MT (with 20 cysteines) [18], two, essentially noninteracting metal binding domains have been proposed based on the spectroscopic and X-ray diffraction evidence [1–7,16,19–21]. The elucidation of the structures of the metal binding sites in the mammalian metallothioneins from NMR and X-ray diffraction techniques [6,7,19–21], and in the crab [21] and lobster [19] metallothioneins from ^{113}Cd NMR techniques, has provided a significant stimulus to studies that are currently examining the dynamics of how the protein interacts with compounds other than metals. For example, studies of competitive ligand reactions or reactions that occur directly with the cysteinyl sulfurs [22–27], competitive metal binding reactions [28–32], metal exchange within metallothionein and between different protein molecules [27,33–36], cellular antioxidant activity [37], anticancer activity [38], intervention in metal-based drug therapy [39,40], and electron transfer reactions [41,42] using a wide variety of chemical and spectroscopic tools have all been reported recently.

Two special properties of metallothioneins make these proteins of particular interest to biochemists and bioinorganic chemists alike. First, is the unusually wide

occurrence of the protein. Proteins that fit the description of a metallothionein have been isolated and characterized from, amongst other sources, fungus, yeast, plants, crustaceans, as well as mammals [1,2,4,5]. Second, metallothioneins are isolated naturally containing essential metals, for example, zinc and copper, as well as toxic metals like cadmium and mercury [43,44]. From a bioinorganic chemistry perspective, the possible properties of a metal–thiolate clustered binding site that involves both terminal and bridging thiolate groups, that binds a number of metals, metals as diverse as Ag(I), Au(I), Bi(III), Cd(II), Co(II), Cu(I), Fe(II), Hg(II), Pb(II), Pt(II), Tc(IV), and Zn(II), is both intriguing and exciting. In this review, I will focus on the metal binding properties of the protein and spectroscopic techniques used to elucidate both stoichiometric, structural, and chemical information. Primarily, I will describe the characterization of the metal binding site in mammalian metallothionein in terms of the metals bound, the stoichiometry of metal to protein, and the possible geometry in the metal binding sites, illustrating and cataloguing progress in elucidating structural and electronic parameters with a variety of spectroscopic tools.

Progress in the determination of the properties of the metallothioneins has been recorded in a series of monographs and reviews that have been published at intervals over the last 15 years. Three international conferences devoted entirely to metallothioneins resulted in volumes of proceedings containing a rich variety of papers covering all aspects of the properties of metallothioneins from a number of sources [1,2,4]. A flavor of the variety of research currently underway is found in *The Metallothioneins,* edited by M.J. Stillman et al. [3]. This book comprises a set of chapters that cover the induction, isolation, quantitation, and characterization of the protein; a description of the detailed X-ray structure determination by Stout and coworkers [7] includes color plates of the three-dimensional structure of Cd_5, Zn_2-MT. Okada, Isobe, and coworkers, also describe details of the formation, and the use of mass spectral data for characterization, of synthetic peptides that can be used to model the metallothionein fragments [45,46]. Copious data on model inorganic metal–thiolate compounds are reviewed by Dance and Dean [47,48]. Many of the techniques used in the study of metallothioneins have been described in *Metallobiochemistry, Part B, Metallothionein and Related Molecules, Vol. 205* of the series *Methods in Enzymology* [5]. Recent spectroscopic properties of the Ag(I), Au(I), and Cu(I) containing proteins are summarized in a review by Stillman et al. [49].

2. Biochemical properties

Metallothioneins have been isolated from an extraordinarily wide range of organisms [1–5]. In many cases, concentrations of the protein can be dramatically increased by induction with one of a number of agents. Many metal salts will induce synthesis of the protein, in some cases the inducing metal will bind to the protein, in other cases the zinc or copper-containing protein will be synthesized. In addition, stress, starvation, organic solvents, steroids, have all been shown to exhibit induction properties usually of the zinc or copper containing protein in mammals, fish, crusta-

ceans, and plants. However, this unusual yet rich chemistry lies outside the scope of this review. The following papers provide examples of some of the experimental evidence for different forms of induction [50–55]. Metallothionein induction has also been reviewed in detail in the recent series of volumes [1,2,4,56]. The genetic origin of the metal-induction of metallothioneins has been elucidated, for example, see [57,58], and Winge and Dameron [59].

Three classes of metallothionein have been identified to date (for a detailed summary and complete sequences of a wide range of metallothioneins, see Kagi [18] and Kojima [60]. Class I proteins cover the mammalian peptides, with typically 60–62 amino acids, complete correspondence between the cysteine locations, many cys-x-cys (where x is a noncysteine residue) units, and also a number of cys-x-x-cys units. The complete absence of aromatic amino acids is an important and characteristic property of these peptides, that has significant ramifications with respect to possible spectroscopic probes. As we see below, optical spectroscopy is able to provide spectral data for thiolate to metal charge transfer transitions that occur between 220 and 350 nm, a region that would be completely masked by the presence of aromatic groups. The available structural chemistry of a number of metallothioneins from a variety of sources is currently based heavily on the detailed results from both NMR (^{111,113}Cd and ^{1}H) and X-ray experiments carried out on the mammalian protein [2,6,7,16,20]. In the studies on mammalian protein, the N-terminal is named the β metal binding domain, in which, for Zn(II) and Cd(II), the M_3S_9 cluster forms, and the C-terminal is named the α domain in which the M_4S_{11} cluster forms with Zn(II) and Cd(II)[3]. A shorter list of class II metallothioneins has also been assembled by Kagi [18]. These peptides occur in sources quite different from mammals, e.g. yeasts, and fungus. Considerable information is now also available concerning metal binding and the structures of the metal binding sites for these proteins. In particular, EXAFS [61] and NMR [62] studies have been reported that describe models for the metal–cysteine connectivities in both the copper and silver substituted yeast metallothionein. These data support a proposal from the EXAFS studies [61] that metal binding in these class II proteins, which have only about half the number of cysteines of class I peptides, involve a clustered metal–thiolate structure in a single domain that has a M_8S_{12} core [62].

Finally, the class III peptides comprise the γ-glutamyl cysteinyl isopeptides ($\gamma\gamma$-EC peptides). These peptides are found in a range of sources, including yeasts (for example, *Schizosaccharomyces pombe)* and plants, and bind Zn(II), Cd(II), and Cu(I) [63–65]. Hayashi and Winge [66] provide a very complete description of the synthesis, characterization (including mass spectral data), and chemical properties of the γ-EC peptides.

Identifying possible biological functions of metallothioneins in general (i.e. classes

[3] The only structures for which the binding site metal–thiolate connectivities and metal coordination geometries are known are Cd_5Zn_2-MT for which a crystal structure has been reported [6,7] and a number of proteins containing Cd(II), and a few where both Zn(II) and Cd(II), in which analysis of ^{113}Cd NMR data complemented by ^{1}H NMR techniques, have been used in the determination of the three-dimensional structures [16,20], see also Table 2.

I and II) has been an active topic for discussion since the first reports by Vallee et al. [1–5,8–11]. The relationship between the tissue concentrations and toxicity of a range of Group 11 and 12 metals (especially Cd(II), Cu(I), and Hg(II) [44,67–69]), and the implications for the presence of metallothionein in the livers of patients suffering from Wilson's disease [70,71], has long been used to support roles in metal detoxification and metal homeostasis for the metallothioneins. However, the significant number of other induction stimuli and the wide occurrence of metallothioneins suggests that these may not be the sole or even the primary physiological roles of the protein. A number of comprehensive reviews of the possible biological functions of each class of metallothionein have appeared recently; the one by Cherian and Chan provides an excellent and up to date source of information on the possible biological functions [56]. The Third International Conference on Metallothionein [4], was convened to examine the medical aspects of the role of metallothioneins in biological systems, for example [72–75]. Recently, high concentrations of apometallothionein have been detected in a range of tumor cells from mice and rats [76].

Extensive details of current techniques for the induction, isolation, purification, and quantitation of a wide range of metallothioneins have been described recently by Suzuki [77] as well as in a number of chapters in *Metallobiochemistry* [5].

3. Primary sequence

The most complete summary of the primary sequence of a wide range of metallothioneins that fall into classes I and II has been recently compiled by Kagi [18]. For the purposes of spectroscopic and structural studies, the key and quite unique feature of the metallothioneins is the presence of such a high fraction of cysteinyl sulfur that can bind as the thiolate. The absence of disulfide bonds means that the three-dimensional structure in metal-free metallothionein is essentially that of a random chain. In the mammalian protein 20 cysteinyl sulfurs (S_{cys}) out of a total of between 60 and 62 amino acids in the peptide are available for coordination to metals. Fig. 1 shows the sequence of the 62-amino acid rabbit liver MT 2a as described by Kagi [18]. The formation of S_{cys}–M–S_{cys} bonds crosslinks the peptide, much like disulfide groups, resulting in formation of a metal binding site enclosed by the hydrophilic envelope of the peptide chain. In the cadmium-containing mammalian metallothionein (Cd_7-MT), the two cadmium–thiolate clusters involve 8 bridging thiolates and 12 terminal thiolates. The three-dimensional structure calculated by Stout's group [6,7] clearly shows how the metals in these two clusters are insulated from the environment by the peptide chain with the exception of two deep crevices that provides direct access to the metal–thiolate structures in each domain [6,7]. Fig. 2 shows a representation of the three-dimensional structures of the α and β binding domains in the 62 amino acid, 20 cysteine, rabbit liver MT 2a; this diagram of the structure of Cd_7-MT 2a is based on the connectivities established by NMR and X-ray results [6,7,16,20]. No three-dimensional structure similar to that shown by Stout et al. [6,7] using space filling atoms has been published for any other metallothionein to date based on structural studies. However, a minimized structure for

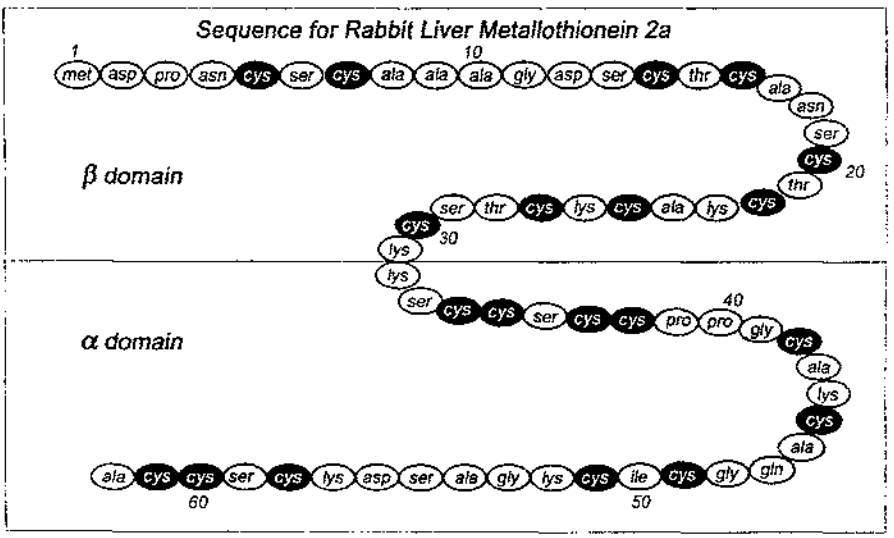

Fig. 1. Amino acid sequence of rabbit liver metallothionein isoform 2a. Cd(II) and Zn(II) bind in two domains, named α and β, that are associated with 31 residues of the N-terminal and, for isoform 2a, also 31 residues of the C-terminal, respectively. The diagram shows the distribution of the nine cysteines in the β domain and the 11 cysteines in the α domain. Drawn using data of Kagi [18].

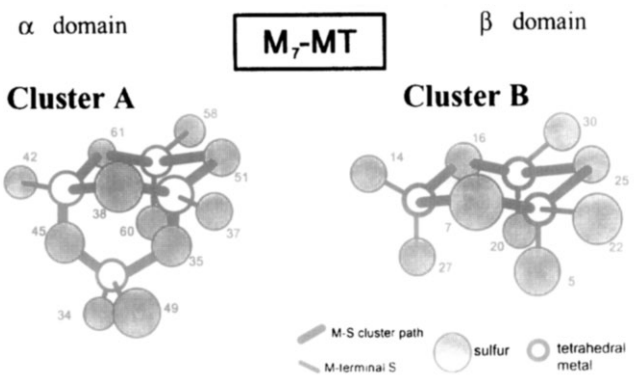

Fig. 2. A representation of the three-dimensional structures of the two metal binding domains identified by ^{113}Cd and ^{1}H NMR, and X-ray diffraction techniques for Cd_7-MT 2 [6,7,16,20]. The numbering scheme refers to the location of the cysteines in the 62-amino acid primary sequence of rabbit liver MT 2a (from data reported by Kagi [18]).

rabbit liver Cu_{12}-MT from a molecular modeling calculation has been reported from my laboratory by Anthony Presta in collaboration with Herman Zinnen at CAche (Beverton, Orgeon, USA), based on spectroscopic measurements made during titrations of Cu(I) into a solution of rabbit liver Zn_7-MT [78,79]. Like the structure of Cd_5Zn_2-MT determined by Stout [6,7], crevices are found in each domain of the three-dimensional representation of the structure. NMR studies have played a key

role in the determination of the overall structures in metallothioneins of both class I and II, first using ^{113}Cd NMR techniques, then ^{1}H 2D techniques [16,19–21,80–83]. Currently, EXAFS data (as described below and in Table 1) are providing precise bond lengths and coordination numbers to complete the structural puzzle.

The similarities between a large number of metal–thiolate clusters formed from inorganic thiolates and the structures formed in the metallothioneins should be mentioned. Dance has recently reviewed the extensive metal–thiolate coordination chemistry [47]. Structural studies by Carty and coworkers are of direct interest when considering the structural properties of mercury–thiolates [84]. Generally, synthetic inorganic complexes of Ag(I), Cd(II), Cu(I), Hg(II), and Zn(II) with thiolate ligands provide structural information that can link bond lengths with coordination geometries, see for example, Pickering et al. [85] and Stillman et al. [49].

4. Metal binding properties

A major thrust of studies into the properties of metallothioneins followed reports concerning the toxicity of cadmium to humans. These reports described a link between dietary cadmium intake and physiological levels of metallothionein, for example, [69,86–92], and especially details of the toxicity of cadmium to human kidneys. Cadmium has entered the water supply and food chain through a number of routes, and toxicological and pathological studies have identified a range of toxic responses in humans [69,86–88,93]. The first major toxicological incident that has been described in detail involving cadmium is that of itai itai disease in Japan [94]. Later research showed that stimulated levels of metallothionein were associated with the elevated cadmium levels, which led to a proposed role for mammalian metallothioneins in detoxifying cadmium [44]. Wilson's and Menkes' diseases, diseases that involve incorrect metabolism of copper, have also been associated with metallothionein through copper(I) binding reactions [96–100].

Today, although many roles have been suggested for metallothioneins, the most important factors from a bioinorganic chemistry viewpoint are the wide ranging metal binding properties exhibited by each of the three classes of protein. The most significant chemical property of the metallothioneins may be the formation of the metal–thiolate cluster structures involving as many as 18 metals and 20 cysteinyl thiolates (for example, the formation of Hg_7-MT 2, Hg_{11}-MT 2, and Hg_{18}-MT 2 from rabbit liver [101–104]), with the metals bound in one or two domains. The essence of studies of the metal-related structural chemistry is to determine the metal to protein stoichiometry, the coordination geometry around the metals and associated bond lengths. These data will lead to predictions of the three-dimensional structure that forms from the RS–metal–SR cross-linked peptide (as in the studies that led to the complete description of rabbit liver Cd_7-MT [6,16,20]). While optical spectroscopic techniques can provide essential parts of the puzzle, in particular, the metal to protein stoichiometries, the major challenge remains with NMR, X-ray

Table 1
Examples of the spectroscopic aspects of metal binding to metallothioneins. A limited selection of metals studied and spectroscopic techniques used is shown

Metal	Origin	Reported MT species and spectroscopic techniques used
Ag(I)	Rabbit liver	Absorption: Zelazowski and Stillman [119] report on speciation that occurs as Ag(I) is added to Zn_7-Mt 2 at a range of temperatures. CD: Zelazowski et al. [118,119] illustrate that the structural chemistry for Ag-MT is dominated by the formation of the Ag_{12}-MT 2 and Ag_{18}-MT 2 species. Later studies of Gui et al. [178] show that isoform 1 forms Ag_{12}-MT and Ag_{17}-MT. EXAFS: The Ag_{12}-MT and Ag_{18}-MT species exhibit almost identical bond lengths for Ag-S, 244 ± 3 pm from sulfur K-edge EXAFS [178]. XANES data have been reported for the Ag_{12}-MT and Ag_{18}-MT species [178]. Emission: Ag_n-MT (n = 1–20) emits light in the 560 nm region when frozen glasses of the protein (77 K) are excited near 300 nm [31,118,127,128].
	Neurospora crassa	^{1}H: Chemical shift assignment for 25 amino acid peptide chain [62].
Cd	Rabbit liver	Absorption, CD and MCD spectra recorded as Cd(II) was titrated into the two fragments (α and β), apoMT, and Zn-MT provided a detailed view of Cd(II) binding in mammalian metallothionein, as the spectral data could be interpreted in terms of a distributed model, in which Cd(II) bound to both domains first, then rearranged to the domain specific structure [29,30]; similar conclusions were reached independently by Willner et al. [244]. The temperature dependence in the metal binding reaction was evident directly from the set of CD spectra and provided evidence that at low concentrations (10^{-5} M) Cd(II) bound to form a kinetic product. Unlike the naturally isolated Cd_4, Zn_3-MT, the Cd(II) occupied both domains, only forming the Cd_4^a, Zn_3^b-MT following equilibration [29]. See also below for NMR results for similar reactions and the section of metal binding dynamics and Cu(I) binding for further discussion on metal binding dynamics. The MCD spectrum is sensitive to the coordination geometry of the chromophore, a distorted Faraday A term is observed for Cd_7-MT [30] compared with the highly symmetric derivative signal observed for the tetrahedral CD(II) in $Cd(BAL)_4$. EXAFS data have provided Cd-S bond lengths and coordination numbers, for example, from Jiang et al. [104] the average Cd-S = 250 pm, and the coordination number = 4.2 ± 1.2. XANES [223]. ^{113}Cd NMR data provided the first definitive evidence for a 2-domain structure: M_3S_9 and M_4S_{11} [16]. ^{1}H-^{113}CD-NMR data allowed calculation of the correct amino acid sequence of rabbit liver Cd-MT, and the cysteine-Cd(II) connectivities [195]. ^{1}H-^{111}Cd-NMR data have been used to study the dynamics of Cd(II) binding, in particular the mechanism for the exchange of Cd(II) between two MT molecules in particular, when Cd_7-MT and Zn_7-MT are mixed the NMR data indicated direct formation of the naturally-occurring Cd_4^a, Zn_3^b-MT following equilibration [33,35]. ^{113}Cd NMR, α fragment, Cd_4S_{11}, [224].

Table 1 (*continued*)

Metal	Origin	Reported MT species and spectroscopic techniques used
	Rat liver	Cu, Zn-MT: ^{113}Cd NMR, using substitution of Zn(II) by Cd(II) to show that the Cu(I) was located in the β domain [264,17].
	Calf liver	^{1}H NMR, 3-D structure proposed; chemical shifts for amino acid residues [80].
	Human	^{113}Cd NMR, 2, distinct, 3-metal Cd-Scys clusters; equivalent to two β domains [21].
	Scylla serata crab	Absorption spectra of Cd_5, Cu-MT and Cd_6-MT [26].
	Lobster	^{111}Cd, NOESY and TOCSY 2D NMR spectra reported for Cd_6-MT; Cd-cysteine connectivities determined [19].
Cu(I)	Rabbit liver	Extensive CD and emission spectra have been reported for Cu(I) binding to apo-MT and Zn_7-MT, for example [27,78].
	Neurospora crassa	^{1}H NMR study of Cu-MT [83].
	Saccharomyces cerevisiae	Emission at 609 nm corresponds to that reported for other copper metallothioneins [171].
Co	Horse kidney	Absorption and MCD spectra of Co-MT 1a between 240 and 850 nm that show both d-d transitions (600–800 nm) and charge transfer transitions (250–450 nm) provide unambiguous evidence for tetrahedral coordination of the Co(II) by the cysteinyl thiolates (196].
	Rabbit liver	Absorption, CD, MCD and EPR studies of Co(II) binding to apo-MT 1 indicate tetrahedral coordination of Co(II) by thiolates [197]. Study of the dependencies of the absorption and EPR signals on the Co(II) to apo-MT 1 molar ratio showed that cluster formation occurred when 4 Co(II) atoms had been added [198]. Absorption, CD, MCD and EPR studies of Co(II) binding to apo-α MT indicated tetrahedral coordination of 3 Co(II) by 9 rather than all 11 thiolates in the fragment; this binding pattern was unlike that in Co_7-MT 1 [199]. ^{1}H NMR studies of Co_7-MT 2 show protons associated with a well defined Co_4-α-domain, but not the Co_3-β-domain [200,251]. Absorption, MCD, and EPR study of the structures of mixed Co(II)/Zn(II) complexes bound to apo-MT 2 [201,202]. 2-dimensional ^{1}H NMR study of rabbit liver Co_7-MT [203].
	Cancer pagurus crab	Absorption, CD, MCD and EPR for the Co(II) substituted apo-MT [150].
Fe	Rabbit liver	Absorption and MCD spectra showing formation of the Fe_7-MT species [204]; variable temperature MCD and EPR spectra [205]. Mossbauer studies of Fe(II) coordination [206–208] has led to assignment of the structure of Fe_7-MT to one that closely resembles that of Zn_7-MT, in which 4 diamagnetic Fe(II) in the α domain are antiferromagnetically coupled, while 3 Fe(II) in the β domain are responsible for the paramagnetic signal observed; a magnetic moment of 8.5 BM was reported.
	Yeast	Mossbauer studies of Fe(II) coordination in yeast metallothionein by Ding et al. [208] suggest a structure in yeast that involves high spin Fe(II), the 4 diamagnetic Fe(II) are antiferromagnetically coupled.
Hg	Rabbit liver	Absorption: Johnson and Armitage [192] report a detailed study of speciation that occurs as Hg(II) is added to Cd-MT. CD: the spectral titration studies of Lu and Stillman [101–103] illustrate a complicated

Table 1 (*continued*)

Metal	Origin	Reported MT species and spectroscopic techniques used
		structural chemistry exists for Hg-containing metallothioneins; The coordination geometry of the Hg(II) is influenced by the metal ion displaced in competitive titrations. MCD: the MCD spectrum is sensitive to the coordination geometry of the chromophore, a distorted Faraday A term is observed for Hg_7-MT [102] compared with the highly symmetric derivative signal observed for the tetrahedral Hg(II) in $Cd(BAL)_4$ [114]. EXAFS: For Hg_7-MT 2, Hg-S = 233 ± 2 pm with CN = 1.8 ± 0.5; the conclusion was that long range coordination by sulfur was not detected by the EXAFS technique but leads to the increase in error on the coordination number [104]. For Hg_{18}-MT 2, Hg-S = 241 ± 1 pm with CN = 1.9 ± 0.2; here a chlorine is detected at 257 pm with a CN = 0.61 and a degree of disorder [104]. XANES: Reported for Hg_7-MT 2 and Hg_{18}-MT 2 [223].
Ni	Rabbit liver	Absorption, CD, and MCD studies of Ni(II) binding to apo-MT 1 indicate tetrahedral coordination of Ni(II) by thiolates [197].
Tc	Rabbit liver	Absorption spectra for $(TcO)_n$-MT, n = 1–7 [226,245].
Zn	Rabbit liver	EXAFS data provide very precise data on the Zn–S bond lenths in Zn_7-MT, for example, Zn–S = 234.9 ± 0.07 pm, CN = 4.2 ± 1.2 [104]. XANES [223].
	Human	Comparison of ^{1}H NMR signals of human Zn_7-MT and Cd_7-MT to correlate the three-dimensional structure of the Zn-protein with the previously determined structure of the Cd-protein [80].

absorption, and X-ray diffraction techniques to determine metal–sulfur bond lengths, coordination geometries, and finally, overall structures.

4.1. Metal binding in vivo

Naturally occurring metallothioneins are generally isolated with Zn(II) (mammalian) and Cu(I) (yeast and fungus) [18,54,105–107]. The Cd(II) found in mammalian metallothioneins isolated in the absence of induction may be considered to have been bound following the ingestion or inhalation of Cd(II) from an environmental or food source. Although exposure of rats to copper results in the induction of copper metallothionein in the liver, for example [108]. Piotrowski was amongst the first to investigate the range of metal salts that will induce synthesis of mammalian metallothioneins, see, for example [109,110]. In these experiments, the metallothionein that was induced bound either the challenge metal, Zn(II), or Cu(I).

The roles of the several metals in inducing elevated levels of metallothionein in different organs are discussed in detail in *Biological Roles of Metallothionein* [86]. Reports continue to appear comparing the toxicity of various metals and the related induction of metallothionein; for example, Dunn et al. describe a compartmental model for copper metabolism in rats that invokes metallothionein as a temporary sink in the livers [108]. The range of metals that will induce metallothionein is very

wide, including, a recent report that polonium metallothionein can be isolated from rat livers following administration of Po [111]. In terms of medically important metal-based drugs, the gold thiolmalate used in the treatment of arthritis, and the cisplatin used in cancer treatment have received considerable attention [72]. Gold will bind in vivo in rat kidneys, for example, [112]. A protective role of metallothionein has been developed based on prior administration of bismuth when potentially toxic cisplatin is administered [74,113].

4.2. *Metal binding in vitro*

A great many metals will bind to MT in vitro, these include Ag(I), Au(I), Bi(III), Cd(II), Cu(I), Co(II), Fe(II), Hg(II), Ni(II), Po, Pt(II), and Tc(IV)O [1–5,32,114–119]. Generally, two strategies are used when studying the metal binding reactions of metallothioneins in vitro. First, these metals bind directly and readily to the metal-free or apo-protein [5,9,29,30,32,114–121]. In reactions carried out using mammalian metallothionein, the metal free protein can be prepared by gel filtration of the Zn-MT at pH 2, followed by desalting [120]. Apo-MT is air sensitive and precautions must be taken during metal binding studies to ensure that oxidation

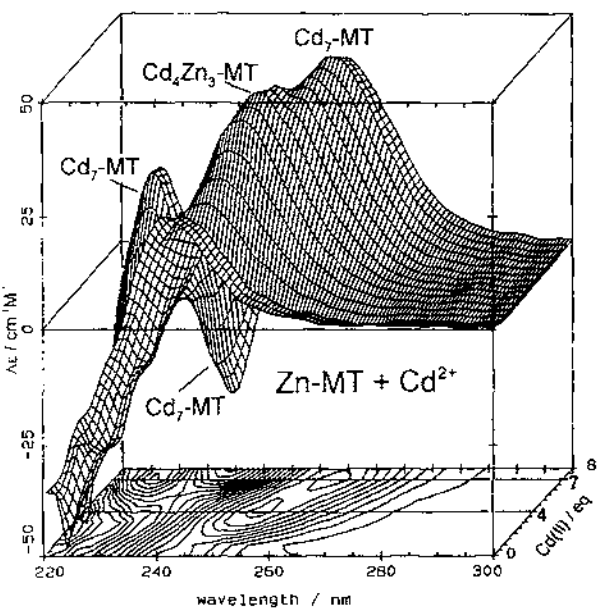

Fig. 3. CD spectra recorded during a titration of rabbit liver Zn_7-MT 2 with Cd(II) at room temperature and pH 7. Aliquots of Cd(II) were added to a 10 μM solution of Zn_7-MT. The CD spectra are plotted as a function (z) of the Cd(II):MT molar ratio. The contour diagram shows the two stages in the reaction, the first at Cd(II):MT = 4 and the second for Cd(II):MT = 7 [30]. Note the overall red shift in the CD band maxima as S→Cd charge transfer bands replace the S→Zn charge transfer bands as the titration progresses. The derivative-like spectral feature that forms between the Cd:MT = 4 and seven points is a signature of the filled Cd_4-α-MT domain. Reproduced with permission from Ref. [78].

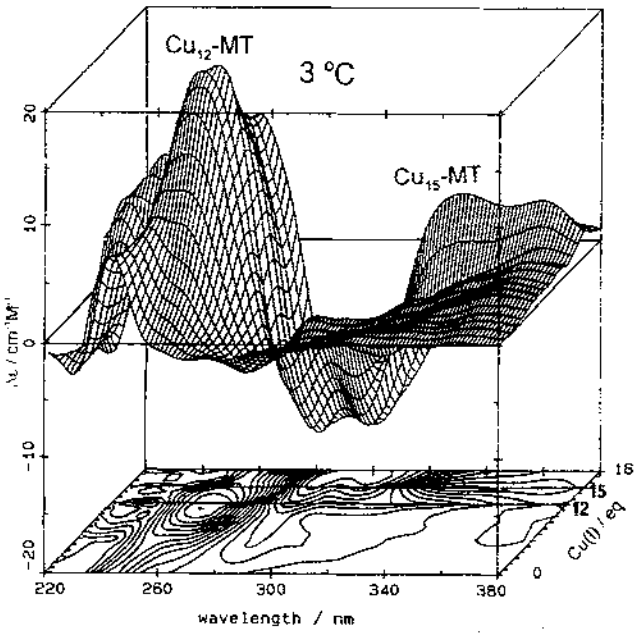

Fig. 4. CD spectra recorded during a titration of rabbit liver Zn_7-MT 2 with Cu(I) at 3 °C and pH 7. At this temperature the spectral features of the Zn_7-MT are gradually replaced by the spectral signature of Cu_{12}-MT, followed by formation of Cu_{15}-MT, before the peptide chains unwinds at higher Cu(I):MT molar ratios. Reproduced with permission from Ref. [78].

of the cysteines to cystines does not occur. Because the binding constants for metal binding to the metallothionein cysteinyl thiolates follow the general order found for inorganic thiolates, $Hg(II) > Ag(I) \approx Cu(I) > Cd(II) > Zn(II)$, if Zn_7-MT is used at pH > 6, then the Zn(II) will be displaced by incoming metals with greater binding constants. Optical techniques, including absorption, emission, magnetic circular dichroism (MCD), and particularly, circular dichroism (CD), have provided a wealth of information about changes that take place in the metal binding site as metals are added to either apo-MT or Zn_7-MT [17,27,29–32,49,78,79,126–139]. We show as examples a number of sets of CD spectra: in Fig. 3 for Cd(II) binding to Zn_7-MT 2, in Figs. 4 and 5 for Cu(I) binding to Zn_7-MT 2, in Figs. 8–12 for Hg(II) binding to either the apo-MT or to Zn_7-MT 2, and in Fig. 13 for Ag(I) binding to apo-MT. Figs. 6 and 7 show the sensitivity of the optical emission spectrum towards Cu(I) binding to Zn_7-MT 2. Fig. 14 compares the CD and MCD spectra recorded for the same set of solutions of Hg-MT, prepared by adding Hg(II) to apo-MT. Some of the spectroscopic properties of the metallothioneins are referred to in Tables 1–4.

Because the Zn(II) in Zn_7-MT is tetrahedrally coordinated by the thiolate groups, considerable reorganization must occur in the binding site to accommodate metals like Cu(I) and Ag(I), metals that generally exhibit trigonal or digonal coordination geometries. The CD technique is very sensitive to changes in the orientation of the peptide chain as a whole. The reorientation of the peptide chain induced by a switch

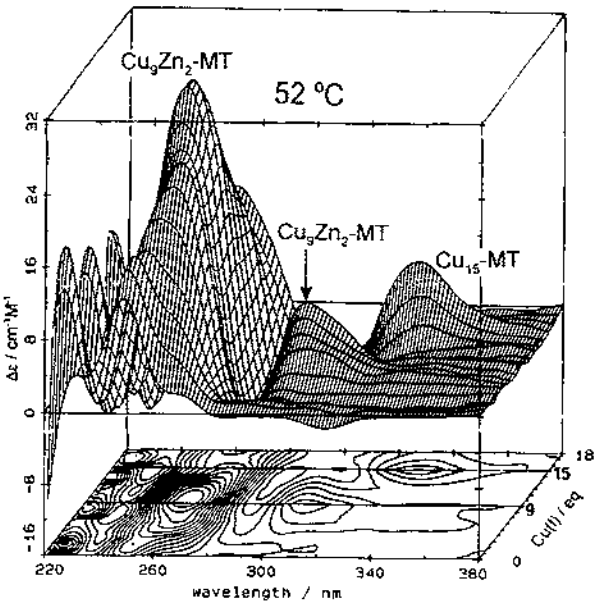

Fig. 5. CD spectra recorded during a titration of rabbit liver Zn_7-MT 2 with Cu(I) at 52 °C and pH 7. At 52 °C a new species, namely Cu_9Zn_2-MT forms with a unique and intense CD spectral pattern. The CD spectrum of Cu_{12}-MT is obscured by the strong bands associated with Cu_9Zn_2-MT. The elevated temperature allows formation of a species not accessible at 3 °C. Cu_{15}-MT subsequently forms before the peptide chain unwinds under the influence of a Cu(I):MT molar ratio > 16. Reproduced with permission from Ref. [78].

in coordination geometry from tetrahedral to trigonal results in dramatic changes in the chirality of the binding site as a whole. The associated changes in the CD intensity during titrations of Zn-MT with other metals shows that a number of structures form as the molar ratio of the incoming group increases and the initially-bound metal is displaced, for example [17,78,102,121]. While major changes to the optical spectrum cease at the Cd(II):MT = 7 point when Cd(II) is added to Zn_7-MT [30], a series of changes is observed when other metals bind to Zn-MT past the 7 point. However, the coordination chemistries involved for Ag(I) [119], Cu(I) [27,78], and Hg(II) [102] are considerably more complicated than for Cd(II) and Zn(II). In these cases it is suggested that both intermediate, mixed-metal species, and species involving a change in coordination number result in the observation of several saturation points in the optical spectral data.

4.3. Selected metals

4.3.1. Cadmium and zinc

The mixed metal Cd, Zn-MT, and the single metal Zn_7-MT and Cd_7-MT mammalian metallothioneins have been widely and continuously studied since the 1960s [1]. This is not surprising when one considers that the first well-defined metallothion-

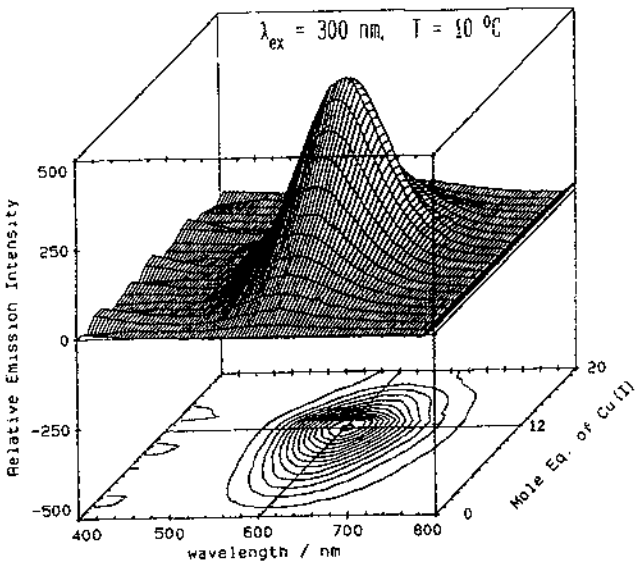

Fig. 6. Emission spectra recorded during a titration of rabbit liver Zn_7-MT 2 with Cu(I) (A) at 10 °C and pH 7. Aliquots of Cu(I) were added to a 10 μM solution of Zn_7-MT 2. Excitation at 300 nm results in the characteristic emission spectrum of rabbit liver Cu-MT at room temperatures: a large Stoke's shift, a band maximum near 600 nm, and a non-linear change in emission intensity as a function of the Cu(I):MT molar ratio. The intensity in this figure has been normalized for the number of Cu(I) added. Note that the increase in emission intensity at 600 nm is roughly linear between 1 and 12 Cu(I) added, then the intensity gradually diminishes with the addition of further Cu(I). Reproduced with permission from Ref. [27].

eins contained both cadmium and zinc [9,10]. At the same time research into cadmium toxicity to humans was also extensive, for example [86–88], and the role of metallothionein in binding cadmium was clearly significant. A considerable amount of optical and NMR data have been reported for cadmium-containing metallothioneins [1,2,10,16,20,21,80,81,122–124]. The two metal binding domains in mammalian Zn_7-MT and Cd_7-MT, which are based on metal–thiolate clusters with stoichiometries of M_3S_9 and M_4S_{11}, were elucidated from analysis of ^{113}Cd and ^{1}H NMR spectra, together with results from chemical techniques [16,20,81,122]. In the invertebrate crab and lobster metallothioneins, the ^{113}Cd NMR data for Cd_6-MT have been interpreted in terms of two domains with the same metal to sulfur stoichiometry as the β domain in rabbit liver metallothionein, namely M_3S_9 [19,21]. In the class II metallothioneins, those isolated from yeasts and fungus primarily, a single domain has been proposed, for example, from the analysis of the ^{1}H–^{109}Ag NMR data of Ag-MT [62]. Although the NMR studies have provided perhaps the most continuous and extensive set of data concerning the metal binding site structures in metallothioneins (see Table 2), both optical and NMR techniques have also provided detailed information on the metal binding stoichiometries and metal binding dynamics. For a protein that binds multiple metals, answers to a number of questions are needed. First, how does the first metal enter the metal binding site? Second, how

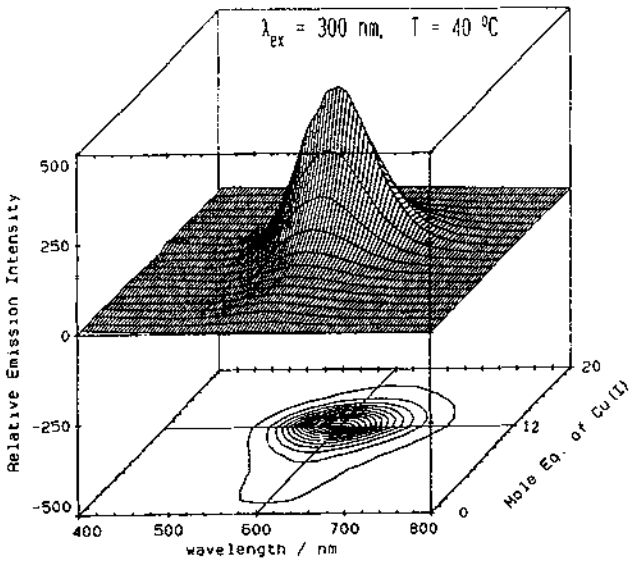

Fig. 7. Emission spectra recorded during a titration of rabbit liver Zn_7-MT 2 with Cu(I) (A) at 40 °C and pH 7. Aliquots of Cu(I) were added to a 10 μM solution of Zn_7-MT 2. Excitation at 300 nm results in the characteristic emission spectrum of rabbit liver Cu-MT at room temperature: a large Stoke's shift, a band maximum near 600 nm, and a non-linear change in emission intensity as a function of the Cu(I):MT molar ratio. The intensity in this figure has been normalized for the number of Cu(I) atoms added. At 40 °C the overall intensity is less than at 10 °C, however, significantly, there is negligible emission intensity between 1 and 6 Cu(I) added. This first phase is followed by a steep rise in intensity to the 12 Cu(I) point. Reproduced with permission from Ref. [27].

do subsequent metals bind? Third, how does metal exchange occur between different sites and different domains? These questions are of significant interest both from the standpoint of the mechanism of the metal binding reactions that take place in vivo and possible competitive metal chelation reactions that occur in vitro.

In addition to the extensive structural studies, the fortuitous availability of the NMR active ^{111,113}Cd isotopes as the key metal in the first studied metallothioneins has allowed metal transfer studies to be carried out using NMR as well as optical techniques. Otvos and coworkers has published several papers over the last 10 years on the mobility of Cd(II) between sites and between different molecules, for example [33–35] (see also below).

Absorption, emission, MCD, and CD spectra provide considerable detail about the stoichiometries for complexes that form as Cd(II) is added to either apo-MT or Zn_7-MT [27,29–32,49,78,79,126–139]. The optical spectrum of Cd-containing metallothioneins is dominated by $S^- \rightarrow Cd(II)$ charge transfer transitions in the 240–270 nm region. Because the metal binding site is formed by the wrapping of the 20 cysteinyl thiolates (in mammalian MT) around the 7 metals, a chiral structure may be formed. From analysis of the CD spectral data recorded as Cd(II) was added to rabbit liver Zn_7-MT 2, Fig. 3, and apo-MT 2, it appears that the major contribution to the CD intensity arises from the 4 Cd(II) located in the α domain. The derivative-

Table 2
Examples of spectroscopic techniques applied to metallothioneins

Technique	Protein studied/comments	Reference
Absorption	Cd-MT, Zn-MT, Hg-MT-spectral deconvolution calculation on the energy of the S→M charge transfer band.	[194]
	Rabbit liver Ag-MT; Ag(I) titration of Zn-MT.	[119]
	Rabbit liver Cd-MT; titration of Zn-MT.	[30]
	Hg-MT; Hg(II) titration of Cd-MT.	[192]
	Rabbit liver apoMT; and Cd(II), Hg(II), and Zn(II) titrations.	[227]
	Rabbit liver Hg_7-MT.	[246]
	Rabbit liver Pb_7-MT.	[246]
	Rabbit liver Bi_7-MT.	[246]
	Chinese hamster Cd-MT; dependence of the absorption on the pH.	[247]
	Rat liver apometallothionein and the α and β fragments: absorption, CD and emission spectra recorded during titrations with Cu(I).	[14]
Circular dichroism	Rabbit liver Cd_7-MT; Cd(II) titrations of apo-MT, Zn-MT, α and β fragments. Dynamics of Cd(II) binding as a function of temperature, pH and presence of EDTA.	[29,30]
	Rabbit liver Ag_{12}-MT/Ag_{18}-MT; Ag(I) titrations of apo-MT, α and β fragments, and Zn-MT.	[118,119]
	Rabbit liver Hg_7-MT, Hg_{11}-MT, Hg_{18}-MT; Hg(II) titrations of apo-MT, Zn-MT, Cd-MT, α fragment; formation of Hg_{18}-MT.	[101–103]
	Rabbit liver Cu-MT; titration of Zn_7-MT with Cu(I) reveals formation of complexes at Cu(I): MT=9, 12 and 15.	[78]
	Fetal bovine liver Cu_3, Zn_4-MT; significant differences observed between the CD spectra for isoforms 1 and 2.	[149]
	Rabbit liver apoMT; and Cd(II), Hg(II), and Zn(II) titrations. Calculation of the CD band for the lowest energy thiolate to metal charge transfer transition.	[227]
	pH dependence of CD spectra of chicken Cd-MT, Cu-MT, and Zn-MT.	[17]
	Hamster Cd-MT, includes effect of a pH change on both absorption and CD spectra.	[17]
	Rabbit liver Pb_7-MT.	[246]
	Rabbit liver Bi_7-MT.	[246]
	Chinese hamster Cd-MT; dependence of the dichroism on the pH	[247]
	Neorospora crassa Cu-MT; absorption and CD spectra of the apo-NcMT and with Cu(I) added.	[247]
	Yeast Cu-MT	[248]
	Yeast Schizosaccharomyces cerevisiae Cu-MT, probable stoichiometry Cu_7S_{10} (62); CD spectrum of Cu-MT excreted from yeast cells.	[161]
	Scylla serrata, crab Zn_6-MT titrated with 6 Cd(II).	[174]
	Scylla serrata crab Cd_6-MT.	[134]
	Cancer pagurus crab Cd-MT and Co-MT	[137]
	Synthetic human α and β fragment; absorption and CD spectra during titrations of the synthetic fragments with Cd(II) and Cu(I).	[248]
	Rat liver apometallothionein and the α and β fragments: absorption, CD and emission spectra recorded during titrations with Cu(I).	[14]

Table 2 (*continued*)

Technique	Protein studied/comments	Reference
Emission	see Table 3.	
EPR	Cancer pagurus crab Co-MT; titration of apoMT with Co(II) using the signal due to the d^7 Co(II) as a probe of Co–S–Co cluster formation.	[34]
	Co(II) exhibits a characteristic EPR signal that depends on the degree of loading between 1 and 7 Co(II) per MT.	[201]
Magnetic circular dichroism	Rabbit liver Cd_7-MT; Cd(II) titrations of apo-MT, Zn-MT, α and β fragments; detailed temperature dependence of the magnetic circular dichroism of the metal binding.	[30]
	Rabbit liver Hg-MT	[101]
	Ni-MT	[197]
	Rabbit liver Co-MT; titration of Co(II) into apo-MT: EPR, CD and MCD spectral data.	[196,201,202]
	Rabbit liver Fe_7-MT; low temperature MCD and EPR data reported for Fe(II):apoMT up to 10.	[205]
	Rabbit liver Hg_7-MT.	[246]
	Rabbit liver Pb_7-MT.	[246]
	Rabbit liver Bi_7-MT.	[246]
	Rabbit liver apoMT; and Cd(II), Hg(II), and Zn(II) titrations.	[227]
	Rat kidney Cd_4Cu_6-MT (and also absorption and CD spectra as a function of pH).	[154]
	Scylla serrata crab Cd_6-MT.	[137]
	Cancer pagurus crab Cd_6-MT and Co_6-MT.	[150]
IR and Raman	Rabbit liver apoMT 1, Zn_7-MT, and Cd_7-MT. Raman spectra between 350 and 1800 cm^{-1} are shown.	[249]
	Rabbit liver Zn_7-MT, Cd_4-α and Cd_3-β fragments, Tc(III)OMT; Cd-Neurospora crassa. A Raman band near 138 cm^{-1} was measured for each species and assigned as a metal dependent band.	[250]
^{1}H NMR	Human Zn_7-MT, Cd_7-MT; comparison of ^{1}H NMR signals to correlate the three-dimensional structure of the Zn-protein with the previously determined structure of the Cd-protein.	[80]
	Definitive comparison between the structures obtained for rat liver Cd_5Zn_2-MT by crystallography and Cd_7-MT by NMR spectroscopy; the conclusion reached is that the structure is the same in the crystal and in solution.	[20]
	Co_4S_{11} cluster.	[200]
	Rat liver Cd-MT; 2-D analysis of ^{1}H NMR determines chemical shifts of all amino acids.	[82]
	Rabbit liver; 2-D ^{1}H-^{113}Cd-NMR data allowed calculation of the correct amino acid sequence of rabbit liver Cd-MT, and the cysteine-Cd(II) connectivities.	[195,252]
	Yeast Schizosaccharomyces cerevisiae, Ag_7S_{10} analysis of 2D ^{1}H NMR suggests presence of both digonal and trigonal coordination of the Ag(I) by cysteine.	[62]
^{111,113}Cd NMR	Rabbit liver, native Cd, Zn-MT and Cd_7-MT: first description of the two-cluster model of Cd-thiolate binding in mammalian metallothioneins.	[16]
	Scylla serrata crab Cd_6-MT; description of two Cd_3S_9 cluster domains in the binding site.	[21]
	Rat liver Cd-MT:	[81]

Table 2 (*continued*)

Technique	Protein studied/comments	Reference
	Rat liver α fragment, Cd_4S_{11}; identifies the location of the Cd_4S_{11} cluster in the α fragment.	[224]
	^{111}Cd, NOESY and TOCSY 2D NMR spectra reported for Cd_6-MT; Cd-cysteine connectivities determined.	[19]
	Dynamics of Cd(II) binding and metal exchange reactions and formation in vitro of the domain specific product Cd_4^a, Zn_3^b-MT following equilibration of solutions of Cd_7-MT and Zn_7-MT.	[33,35]
XAFS (or EXAFS) Structural data are summarized in Table 4 below	Yeast Cu-MT: Cu–S bond length of 223 pm with a trigonal coordination.	[61]
	β domain of rat copper metallothionein: Cu–S bond length of 225 pm with a coordination of 2.5 by S.	[243]
	Cu and Zn K-edges in pig liver Cu_6Zn_3-MT: Cu–S bond length of 225 pm with CN = 3; Zn–S = 233 pm with CN = 4.	[253]
	Cu-MT from Neurospora crassa: Cu–S bond length of 220 pm, and Cu–Cu distance of 271 pm.	[254]
	Metal-edge EXAFS for rabbit liver Zn_7-MT, Cd_7-MT, Hg_7-MT, and Hg_{18}-MT.	[104]
	CUP2 (ACE1) Cu-binding protein: Cu–S bond length of 227 pm with CN = 2.34.	[255]
	Cd phytochelatin, Cd-γ(EC)$_n$: Cd–S bond length of 252 pm with CN = 4.	[256]
	S. cerevisiae CuMT, S. pombe Cu-(γEC)$_n$, and a number of copper(I) thiolate model compounds: analysis of the data suggest that the fraction of digonal coordination geometry of the Cu(I) is 30% (rat CuMT, Cu–S = 225.5 pm), 30–40% (S. cervisiae CuMT; Cu–S = 225.0–224.2 pm) and 50% (N. crassa CuMT; Cu–S = 225.5 pm).	[85]
	S K-edge EXAFS of Zn-MT, Cd_7-MT, Cu_{12}-MT, Ag_{12}-MT and Ag_{17}-MT 1, together with Zn_4S_{10} and Cd_4S_{10} model compounds, show that the S EXAFS can be used to determine subtle changes in the structure of the binding site, changes not associated with changes in coordination geometry of the metal.	[178]
XPS	Zn-MT, Cd-MT, Hg-MT.	[242]
	Yeast Cu-MT; 932 eV peak supported Cu(I) assignment for the oxidation state of the copper.	[161]
	XPS spectra of metal-electron regions of Zn-MT, Cu-MT, Cd-MT, Hg-MT, and of the S $2p_{1/2,3/2}$ levels of native fetal Cu-MT. Table of electron binding energies for S $2P_{1/2,3/2}$ levels in Cd-MT, Zn-MT, Cd, Zn-MT, Hg-MT and Cu-MT, and also metal complexes of cysteine and cystine.	[17]

shaped CD envelope associated with the Cd_4-α domain can be used as a marker for available sites in the α domain during mixed metal reactions [78,79].

4.3.2. Copper

Copper is an essential element to life forms, frequently occurring with sulfur containing amino acids, because of the significant role for copper in electron transfer,

Table 3
Luminescent metallothioenins

Protein	Comment	Reference
Ag-MT; rabbit liver	Emission and excitation spectra measured at 77 K for; Ag_{14}MT; $\lambda_{ex}=300$ nm, $\lambda_{max}=570$ nm.	[127]
Ag-MT; rabbit liver	Excitation and emission spectra recorded at 77 K during a titration of Zn_7-MT with Ag(I) for n = 1–24, wavelength and intensity dependence of luminescence on Ag:Scys molar ratio; for $Ag_{10}S_{20}$ $\lambda_{ex}=300$ nm, $\lambda_{max}=540$ nm.	[128]
Au-MT; rat liver	Emission and excitation spectra measured at 77 K; $\lambda_{ex}=305$ nm, $\lambda_{max}=600$ nm.	[127]
Cu-MT; rabbit liver	Emission and excitation spectra measured at 77 K for; Cu_6MT; $\lambda_{ex}=300$ nm, $\lambda_{max}=530$ nm.	[127]
Cu-MT; rabbit liver	Excited state lifetimes measured at room temperature for Cu_{12}-MT 2; $\tau=20$ ns, 700 ns, and 3.5 μsec.	[129]
	Study of emission properties during titrations of Zn_7-MT 2 with Cu(I) to form Cu_n-MT, n = 1–20, at room temperature; $\lambda_{ex}=300$ nm, $\lambda_{max}=605$ nm; temperature dependence of the emission intensity indicates site of initial Cu(I) binding to Zn-MT is in both domains; domain specificity observed only following equilibration.	[27]
	Emission and excitation spectra measured at 77 K from Cu-MT 2 prepared from apoMT; $\lambda_{ex}=300$ nm, $\lambda_{max}=530$ nm.	[127]
	Quenching experiments at room temperature (O_2, acrylamide, and Fe(II)); for Cu_{12}-MT 2 at 40°C: $\tau=650$ ns, 3.6 μsec, and 12 μsec.	[42]
	Use of emission spectra to monitor the mobility of Cu(I) atoms between sites.	[211]
Cu-Mt; rat liver; Cu_nS_{20}	In vivo measurement of emission at 77 K directly from tissue following induction of Cu-MT with $CuCl_2$; $\lambda_{ex}=310$ nm, $\lambda_{max}=605$ nm; $\tau_{1/2}=11$, 98 μsec. Lifetime of Cu-MT at 77 K, $\tau_{1/2}=63$, 132 μsec.	[126]
Cu-MT; rat liver; Cu_nS_{20}	Absorption, CD and emission spectra recorded during titrations of native Cd_5, Zn_2-MT 2, apometallothionein, and the α and synthetic β fragments, with Cu(I).	[14]
Cd, Cu-MT; rat kidney; $Cd_4Cu_6S_{20}$	Excitation and emission spectra at room temperature and 77 K; $\lambda_{ex}=260$ nm, $\lambda_{max}=610$ nm.	[154]
Cu, Zn-MT; fetal bovine liver	$\lambda_{ex}=310$ nm, $\lambda_{max}=565$ nm at 283 K; quantum yield = 0.001.	[149,170]
Cu,Hg-MT; rat kidney	The increasing molar ratio of Hg(II) in the three isoforms of Hg, Cu-MT from rat kidney significantly quenched the emission intensity observed at 580 nm at 77 K.	[135]
Cu-MT; recombinant human, rainbow trout	Cu(I) titration of apo-MT from three synthetic metallothioneins, based on genes for human and rainbow trout MT; emission intensity monitored for the range Cu(I):MT = 1–14, at pH 7.0, $\lambda_{ex}=340$ nm, $\lambda_{max}=580$ nm.	[257]
Yeast Cu-MT and Cu-thiolate clusters in yeast CUP1 MT genes	For yeast Cu-MT at room temperature; $\lambda_{ex}=300$–360 nm, $\lambda_{max}=609$ nm; excited state lifetimes measured at room temperature; $\tau=440$ nsec; quantum yield = 0.006. The luminescence intensity was a maximum for 6–7 Cu(I) added to apoMT.	[171]

Table 3 (*continued*)

Protein	Comment	Reference
Cu-MT ascomycetel Neurospora crassa; Cu_6S_7	First report of an emissive metallothionein, 'an orange emission'. $\lambda_{ex}=305$ nm, $\lambda_{max}=565$ nm; quantum yield = 0.033.	[167] [170]
	Emission and quenching (O_2 acrylamide, and Hg(II)) experiments studied; $\tau=10.3$ μsec in N_2 at 10 °C following excitation at 310 nm.	[172]
Cu-MT; synthetic selenopeptide based on the sequence of Neurospora crassa; Cu_6Se_7	Cu-SeNcMT. Emission detected at 395 nm following excitation at 245 nm; absorption (sh. 260 nm) and CD (weak maximum near 245 nm) spectra were also measured.	[258]
Cu-MT; yeast Saccharomyces cerevisiae; Cu_7S_{10}	$\lambda_{ex}=277$ nm, $\lambda_{max}=609$ nm; $\tau=440$ nsec; quantum yield = 0.006.	[171,157]
	CD and emission of Cu_8-MT released from intact yeast cells; also shown was a photograph of fluorescence from single, copper-loaded, yeast cells.	[174]
Cu-MT; Yeast Schizosaccharomyces cerevisiae Cu-MT, probably stoichiometry Cu_7S_{10}	Emission from Cu-MT released from yeast cells; luminescence of whole yeast cells; $\lambda_{max}=610$ nm	[174]
Cu-MT; yeast; Agaricus bisporus; fungus; Cu_6S_7	$\lambda_{max}=565$ nm; quantum yield = 0.014.	[170]
Cu-MT; ACE1 from yeast	$\lambda_{ex}=270$ nm, $\lambda_{max}=610$ nm; excitation and emission spectra shown; absorption and CD spectra included.	[259]
Pt-MT; rat liver	Emission and excitation spectra measured at 77 K for cis-Pt-MT, trans-Pt-MT and Pt-MT; $\lambda_{ex}=305$ nm, $\lambda_{max}=600$ nm (Pt-MT), 620 nm (*cis*-Pt-MT; *trans*-Pt-MT) nm.	[127]

redox, and enzymatic reactions [140]. The liver and kidneys play an important role in the metabolism of copper in mammals [108,141]. Although an essential element, incorrect metabolism of copper is thought to lead to Wilson's diseases. High levels of copper metallothionein are found in the livers of patients suffering from Wilson's disease [71,142]. The occurrence of copper metallothioneins in vertebrate, invertebrate, and eukaryotic sources has been well documented [105,106,108,110,143–148]. Copper binding is common in each class of metallothionein. Within the class I proteins, mammalian liver and kidney metallothioneins can be isolated with both a zinc and copper content, the crustaceans (crabs and lobsters) can be isolated containing both cadmium [26,149, 15] and copper [148–152]. Copper binding in vivo dominates the class II peptides. Copper metallothionein isolated from rat livers contains between 9 and 11 atoms of Cu(I) per molecule of MT, close to the optimal value of 12 found during in vitro titrations [27,78,153]. The administration of cadmium, bismuth or mercury salts to rats results in induction of metallothionein in the kidney that contains both Cu(I) and Cd(II), or Hg(II) or Bi(III) [110,135,154]. Significant information on the mechanism of induction of

Table 4
Examples of structural properties of metallothioneins determined by XAS techniques[a]

Protein	Metal	Coordination number (CN) and and bond length (pm)	Reference
Rabbit liver	Zn_7-MT; Zn K-edge	Zn–S: 233(1) pm; CN = 4S	[253]
	Zn_7MT 2; Zn K-edge	Zn–S: 234.9 ± 0.7 pm; CN = 4.2 ± 0.5 (4S)	[104]
	Cd_7MT 2; Cd K-edge	Cd–S: 250 ± 2 pm; CN = 4.2 ± 1.2 (4S)	[104]
	Hg_7MT 2; Hg L_3-edge	Hg-S: 234.9 ± 0.7 pm; CN = 1.8 ± 0.5 (2S + 2 distant S)	[104]
	Hg_{18}MT 2; Hg L_3-edge	Hg–S: 234.9 ± 0.7 pm; CN = 1.9 ± 0.2 (2S + 1 distant Cl)	[104]
	Zn_7-MT	Zn–S: 233 pm; CN = 4S Zn–S = 410 pm; CN = 1S	[260]
	Cd_7-MT	Cd–S: Cn = 4S CN = 1S – 410	[260]
	PB_7-MT	Pb–S: 265 pm; CN = 2S	[260]
	Hg_7-MT	Hg–S: 242 pm; CN = 3S	[260]
	Ag_{17}, Cd_2-MT	Ag–S: 240 pm; CN = 2S Ag–Ag: 288 pm; CN = 1Ag	[260]
	Cu_6, Zn_3-MT; Cu K-edge	Cu–S: 225 pm; CN = 3S	[253]
	Zn_7-Mt 1; S L-edge	XANES	[223]
	Cd_7-MT 1; S L-edge	XANES	[223]
	Hg_7-MT 1; S L-edge	XANES	[223]
	Hg_{18}-MT 2; S L-edge	XANES	[223]
Pig Liver	Zn_2Cu_5MT	Cu–S: 221 pm; CN = 3S	[253]
Rat liver	Cu_6S_9; β fragment; Cu K-edge	Cu–S,: 225; CN = 3S (Reevaluated Cu–S as 225.5 pm with 30% digonal coordination of the Cu(I) by S (see Pickering et al. Ref. [85]))	[243]
Rat liver	Cd_7-MT; Cd K-edge	Cd–S: 253(2) pm; CN = 4S	[261]
	Zn-MT; x-ray photoelectron spectroscopy (XPS)	Core electron energy levels reported	[241]
	Cd-MT; x-ray photoelectron spectroscopy (XPS)	Core electron energy levels reported	[241]
	Cu-MT; x-ray photoelectron spectroscopy (XPS)	Core electron energy levels reported	[262]
	Hg-MT; x-ray photoelectron spectroscopy (XPS)	Core electron energy levels reported	[241]
Sheep	Zn_7-MT; Zn K-edge	Zn–S: 229(2) pm; CN = 4S	[263]
Yeast ACE1	Cu-MT	Cu–S: 225.8 pm, 30% digonal coordination of Cu(I) by S.	[85]
Yeast Schizosaccharomyces cerevisiae	Cu_8S_{12}; Cu K-edge; S K-edge [note the revised stoichiometry Cu_7S_{10} (62)]	Cu–S: 223 pm; Cn = 3S (Recalculation by Pickering et al. [85]: Cu–S: there was between 30% and 40% digonal coordination of the Cu(I) by S, Cu–S = 224.2–225.0 pm)	[61]

Table 4 (*continued*)

Protein	Metal	Coordination number (CN) and and bond length (pm)	Reference
Neurospora crassa	Cu_8S_7; Cu K-edge	Cu–S: 220; CN = 3–4S Cu–Cu: 271 pm; CN = 1–2 Cu (Recalculated: Cu–S = 223.3 pm with 50% digonal	[254]
Inorganic model compound	$[Cd_4(SPh)_{10}]^{2-}$; S L-edge	XANES	[223]
Inorganic model compound	$[Zn_4(SPh)_{10}]^{2-}$; S L-edge	XANES	[223]
Inorganic model compound	$[Zn_4(SPh)_{10}]^{2-}$; Zn K-edge	Zn–S: 233 pm; CN = 3.9 S Zn–Zn: 403 pm; CN = 3.6 Zn	[242]
Inorganic model compound	$[Cd_4(SPh)_{10}]^{2-}$; Cd K-edge	Cd–S: 254 Pm; CN = 3 S Zn–Zn: 434 pm; CN = 3 Cd	[242]
Inorganic model compounds	$[Cu_4(SPh)_6]^{2-}$; Cu-K edge $[Cu_5(SPh)_7]^{2-}$ $[Cu_5(SPh)_6]^{-}$	Cu–S: 228.2(2) pm Cu–S: 225.8(2) pm Cu–S: 222.9(3) pm: CN = 2.22 S	[85]

*XAFS data shown unless otherwise noted.

copper metallothionein and the role in the regulation of copper in yeasts has been reported from molecular biology [37,106,147,155–158].

Extensive chemical, spectroscopic and structural studies have been published that describe the Cu(I) to MT stoichiometric ratio, as well as a number of optical properties of copper-containing metallothioneins. The coordination geometry of the copper in the binding site has been investigated using XAS techniques [1–5]. Spectroscopic evidence, especially, EPR and XPS data [17,107,159–162], shows that the copper is bound entirely as Cu(I). In the absence of dioxygen, the cysteinyl sulfurs exist as thiolates with no disulfide bonds present. These properties, essential to the integrity of all metallothioneins, must be confirmed in all samples used for structural studies. After the cadmium and zinc proteins, copper metallothioneins of all three classes have been most extensively studied in vitro. Key metal binding properties for metallothioneins isolated from all sources are (i) the metal to sulfur stoichiometry, (ii) the domain preference in the two-domain class I proteins, and (iii) the coordination geometry of the sulfur around the metal. Winge and coworkers have studied each of these properties, in particular, for copper(I) binding, reporting that 6 Cu(I) bind in each domain in mammalian proteins to form the Cu_{12}-MT species [62,125,163]. It was concluded from these studies that Cu(I) binds preferentially in the β domain, whereas Cd(II) binds preferentially in the α domain of mammalian protein [125,163–165].

Copper metallothioneins have been studied by many different spectroscopic techniques, most summarized in Tables 1–4. Weser and coworkers have studied Cu(I)

binding using absorption, CD, and XPS spectroscopies [17,160,161]. In 1985, Nielson and Winge reported the chemical determination of the Cu:MT stoichiometry as 12, proposing that the Cu_{12}-MT species was the major product of the reaction of Cu(I) with mammalian metallothioneins [125]. Figs. 4 and 5 show the complicated metal–thiolate cluster formation that takes place when Cu(I) is added to solutions of Zn_7-MT. These CD data show that the product of the reaction of Cu(I) with Zn-MT depends on the temperature [78]. The discovery by Lerch of the induction of a copper containing protein, identified as a copper metallothionein, from the fungus Neurospora crassa [166] led to the report that copper metallothioneins emitted an orange wavelength light at room temperature in solution. This property subsequently provided an important additional source of information on copper binding in a wide range of metallothioneins [14,27,31,42,116,127,129,149,167–173]. We have tabulated many of the papers describing the luminescence properties of metallothioneins [(Ag(I), Au(I), Cu(I), and Pt(II)] in Table 3.

Figs. 6 and 7 show the series of emission spectra recorded as Cu(I) is added to Zn_7-MT 2 at room temperature. The peak maximum at the 12 Cu(I):MT point confirms that an enclosed three-dimensional structure forms optimally with 12 Cu(I) [27]. Only recently has an interpretation of the complex function of the emission intensity at 600 nm on the Cu(I):MT ratio been proposed [27]. In this scheme, elucidated for copper binding to the two-domain rabbit liver protein, when Cu(I) binds to Zn_7-MT, Zn(II) is first displaced from both domains on a statistical basis at all temperatures. Over time, the Cu(I) redistributes into the β domain forming the domain specific product up to the 6 Cu(I):MT point. The quantum yield of emission at room temperature from the β domain is approximately 20 times less than the quantum yield for Cu(I) bound in the α domain. As a result of this imbalance in quantum yields, we have been able to monitor the redistribution of Cu(I) from the α domain to the β domain in real time [27]. The luminescence of Cu-MT can also be detected directly from mammalian [126] and yeast cells [174,175]. In the former study [126] we measured emission in the 550 nm region at 77 K directly from Cu-MT located in the rat liver cells following induction of Cu-MT by injections of copper salts [126]. Weser and coworkers reported a microscopic image showing the fluorescence due to Cu-MT from yeast cells; the Cu-MT was subsequently released and CD spectra reported [174]. As with the Cd-MT species, CD spectroscopy has yielded detailed information about the Cu(I) to MT stoichiometry [14,17,32,78]. Recent papers from my group have identified a series of different species that form when Cu(I) is added to either apo-MT, Zn-MT (Figs. 4 and 5) [49,78], or to glutathione as a model compound for the copper binding site in metallothionein [176].

Two major isoforms of mammalian metallothionein can be isolated, namely MT 1 and MT 2, where the numbering is determined by the elution order from a DEAE-based column. Several further subisoforms have been separated by HPLC analysis [15,18,177]. Although different biological roles have not been suggested for the two isoforms, different CD spectral data have been reported for the copper-containing metallothionein from bovine fetal liver [149]. Two other reports of spectral data that are dependent on the isoforms of rabbit liver metallothionein have come from

our laboratory for Ag(I) binding [118,119,178] and for Hg(II) binding [101]. These data suggest that the folding of the peptide, the property that is detected by the CD experiment, is influenced to some degree and for some metals by the exact amino acid composition. This is presumably because certain turns in the tertiary structure that are necessary to coordinate the metals are not possible when the amino acid composition is slightly different.

The Cu(I) bound in metallothionein is available for chelation by competitive ligands. For example, Suzuki et al. [179] show that tetrathiomolybdate will mobilize Cu(I) from metallothionein. The tripeptide glutathione also interacts with the copper bound to metallothionein [28,176].

Because of the significance of copper binding in biological systems, copper metallothioneins from many sources have been examined by X-ray absorption techniques, yielding XANES and EXAFS (or XAFS) data. The EXAFS data have provided a number of Cu(I)–S bond lengths and coordination numbers [107], see Table 4. Currently, these studies suggest that the coordination in yeast and mammalian copper metallothioneins is mainly trigonal with Cu–S bond lengths of approximately 224 pm (Table 4). Recent results from our laboratory using S K-edge EXAFS data [178] yield a Cu–S bond length of 225 pm for rabbit liver Cu_{12}-MT with close to complete trigonal coordination of the Cu(I) by the thiolates. Analysis of companion data for Ag_{12}-MT 2 and Ag_{17}-MT 1 [49,178,180] suggests a much greater degree of digonal coordination is present for the Ag(I), as expected from the inorganic chemistry of thiolate complexes of Ag(I) and in support of the results of an NMR study of Ag(I)-MT from yeast [85].

4.3.3. Mercury

The toxicity of mercury to most life forms has attracted wide interest, see for example individual chapters in *Advances in Mercury Toxicity* [181], *Mercury, Mercurials, and Mercaptans* [182], and *The Chemistry of Mercury* [183]. Mercury(II) binds strongly to thiolates forming complexes characterized by distorted tetrahedral, trigonal, and digonal coordination of the Hg(II). In many cases, distant mercury–chloride bonds play an important role in the structures [84,184]. It is not unexpected that Hg(II) also binds strongly to the cysteinyl thiolates in metallothionein both in vivo and in vitro. Although Hg(II) is generally toxic, a number of proteins have been isolated that are induced by the cellular presence of mercury. Included in this list are mercuric reductase, the MerR metalloregulatory proteins for which detailed chemical and structural information is beginning to emerge, see for example, Refs. [185] and [186], and metallothionein [3]. A number of reports describe the presence and isolation of mercury-containing metallothioneins, for example Refs. [187–191]. Spectroscopic studies to date indicate that Hg(II) also forms a number of distinct complexes with rabbit liver metallothionein [101–104]. Structural information about mercury-containing metallothioneins is currently limited to optical and X-ray absorption (XAS, XANES, EXAFS) studies [101–104,114,192]. The absorption spectrum of metallothionein exhibits the red-shift expected for a sulfur to metal charge transfer band when the metal changes from Zn(II) to Cd(II) to Hg(II) [101–103,114,192–194]. In the model compound Hg-[dimercaptopropanol (BAL)]$_4$

the absorption and MCD spectra show maxima clearly resolved at 280 nm [114]; however the exact spectral envelopes observed in the absorption and MCD spectral data of Hg-containing metallothioneins depend on the specific Hg(II) to protein molar ratio and pH of the solution. (I will refer only to rabbit liver metallothionein in this section because the majority of new results are from experiments using only this protein source, often only isoform 2a.)

The optical spectral data sets observed for Hg(II) binding to either apo-MT or Zn-MT are very much more complicated than the comparable data for Cd(II) binding. The set of CD data recorded for Hg(II) additions to apo-MT 2 (Figs. 8, 9, and 10), Zn_7-MT 2 (Figs. 11 and 12), and Cd_7-MT 2 [101–103] can be compared with the similar sets of CD data for Cd(II) added to apo-MT 2 and Zn_7-MT 2 (Fig. 3) [29,30,78]. Johnson and Armitage [192] analyzed the absorption data obtained during titrations of Hg(II) into Cd_7-MT in terms of a series of compounds in which the Hg(II) adopted different coordination numbers. Significantly, they predicted that the Hg(II) in Hg_7-MT formed from Cd_7-MT did not adopt tetrahedral geometry. Now with the availability of EXAFS data, we find that this is indeed the case [104]: the Hg(II) adopts a distorted tetrahedral coordination with a Hg–S bond length of 233 pm. The set of CD data suggest that much of the complexity in the binding of Hg(II) to metallothionein arises from the availability of multiple coordination numbers, thus it is possible for the CN for Hg(II) to change from 4, to 3, to 2. The CD data shown in Figs. 8 and 9 suggest that when Hg(II) is added to apo-MT or apo-α-MT at pH 7, well defined Hg_7-MT 2 or Hg_4-α-MT 2 species

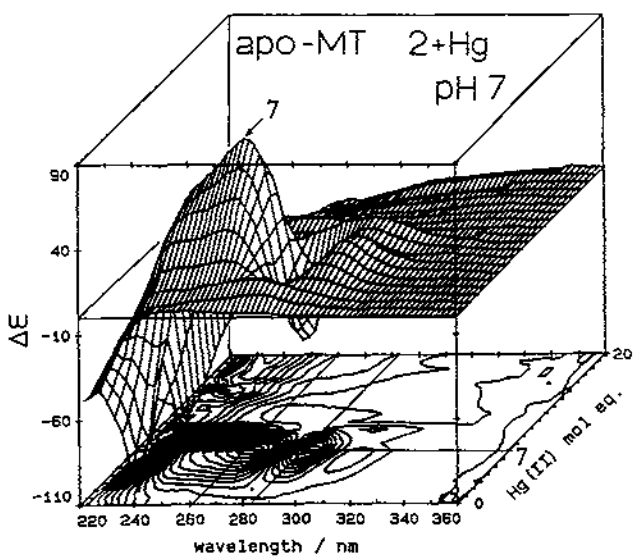

Fig. 8. CD spectra recorded during a titration of rabbit liver apo-MT 2 with Hg(II) at room temperature and pH 7, showing formation of Hg_7-MT 2. Addition of Hg(II) > 7 mole equivalents unwinds the peptide chain; the Hg(II) binds to the protein but no chirality is detected for the binding site. Reproduced with permission from Ref. [102].

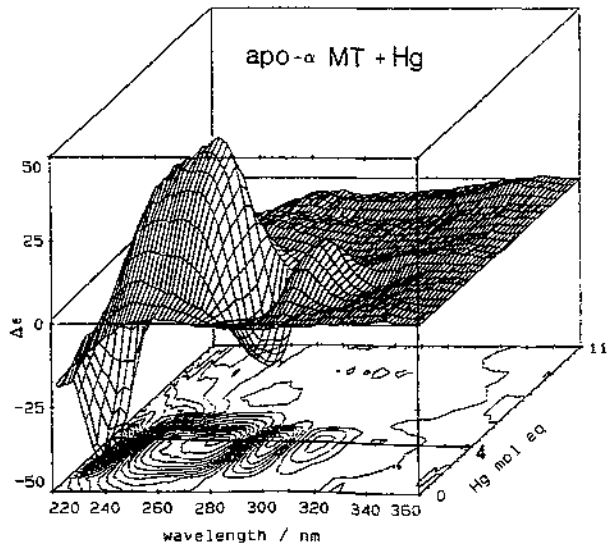

Fig. 9. CD spectra recorded during a titration of rabbit liver apo-α MT 2 with Hg(II) at room temperature and pH 7, showing formation of Hg_4-α MT 2. Reproduced with permission from Ref. [102].

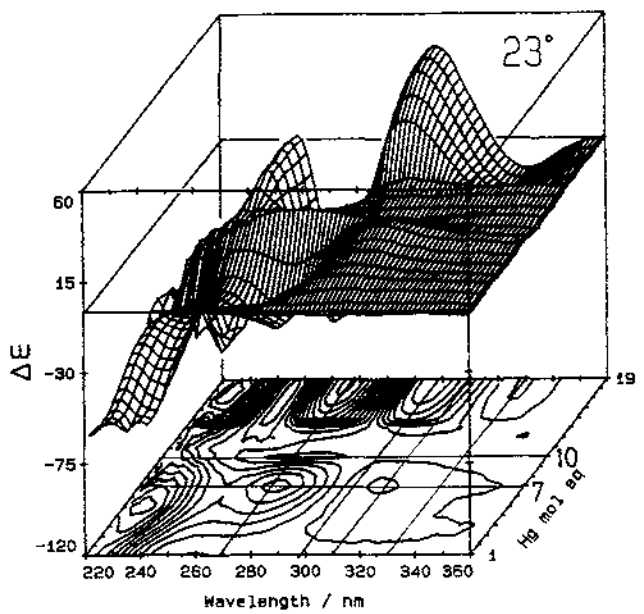

Fig. 10. CD spectra recorded during a titration of rabbit liver apo-MT 2 with Hg(II) at room temperature and pH 2, showing formation first of Hg_7-MT 2, then Hg_{18}-MT 2. Reproduced with permission from Ref. [101].

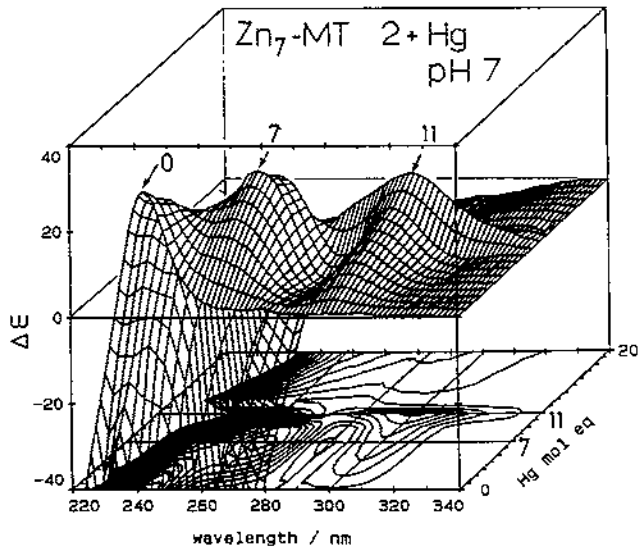

Fig. 11. CD spectra recorded during a titration of rabbit liver Zn_7-MT 2 with Hg(II) at room temperature and pH 7, showing formation of Hg_7-MT 2 and Hg_{11}-MT 2. The effect of the prior presence of the 7 Zn(II) atoms is to allow the peptide to bind the 11 Hg(II) atoms in a well-defined, three-dimensional structure. It is suggested that the coordination of the Hg(II) is close to 4 at the Hg(II):MT = 7 point but 3 at the Hg(II):MT = 11 point. The steep collapse in the CD intensity past 11 Hg(II) indicates that the peptide chain that forms the binding site unwinds at this point in the titration. Reproduced with permission from Ref. [102].

are formed. However, when Hg(II) is added to Zn_7-MT 2 at pH 7 (Fig. 11) a second coordination geometry competes within the binding site so that the CD spectral data saturate at a new Hg to MT ratio of 11, to form Hg_{11}-MT 2. The CD data in Fig. 12 show that the Hg_7-MT 2 species is completely inhibited if the Hg(II) is added to Zn-MT in a solvent containing 50% ethylene glycol, under which conditions only the Hg_{11}-MT forms. At low pH (Fig. 10), Hg_7-MT 2 forms, followed by Hg_{18}-MT 2 [102,103].

5. General structural properties

Over the last 15 years a fairly complete model has been compiled that describes Cd(II), Zn(II), and Cu(I) binding in vitro to crustacean, mammalian, and yeast metallothioneins. The two-domain structure determined from the ^{113}Cd and ^{1}H NMR and X-ray studies for Cd(II) and Zn(II) that involves both terminal and bridging cysteinyl sulfurs [16,122,195] accounts for the overall structure of a number of other metals as determined by a variety of chemical methods and spectroscopic techniques. For example, metallothioneins containing Ag(I), Co(II), Cu(I), Fe(II), and Hg(II) (in addition to Cd(II) and Zn(II)) exhibit spectroscopic signal maxima at metal to protein molar ratios of either 7, for Hg(II) [101–103], Co(II)

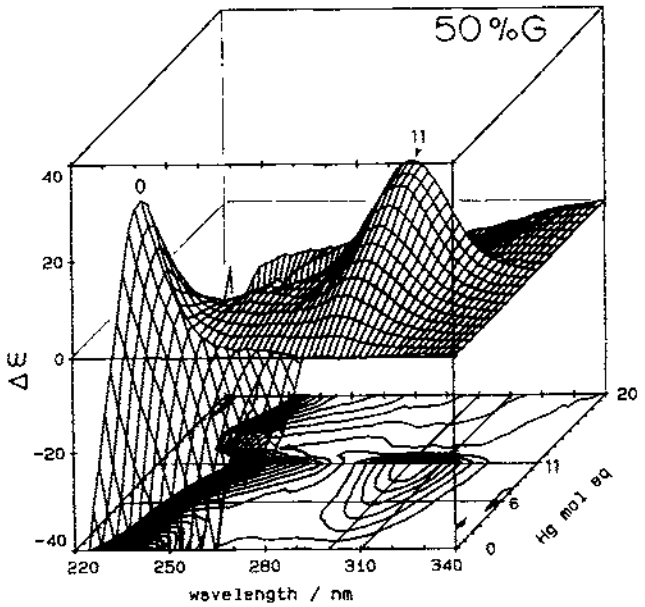

Fig. 12. CD spectra recorded during a titration of rabbit liver Zn_7-MT 2 with Hg(II) at room temperature and at pH 7 in a 50% H_2O/ethylene glycol solvent, showing formation of only the Hg_{11}-MT 2. The strong CD band marked as 0 near 230 nm, is for Zn_7-MT. Reproduced with permission from Ref. [102].

[196–203], and Fe(II) [204–208], or 12, for copper [27,32,78,125] and silver [32,118,119,125,127,128]. Spectroscopic studies of Ag(I) and Hg(II) binding to rabbit liver metallothionein have more recently suggested that $Ag_{17/18}$-MT (Fig. 13) and Hg_{18}-MT (Fig. 10) [101–104,118,119,178,180] also exist as distinct complexes.

5.1. *Binding site specificity*

In a series of papers, Winge and coworkers established that metals bind preferentially to one of the two domains in the absence of a perturbation (the prior presence of a metal, for example when Cu(I) is added to Zn_7-MT) [125,209]. In mammalian metallothionein, Winge and coworkers showed that in the thermodynamically equilibrated protein (we define the product in this way to distinguish it from the kinetic product that is observed spectroscopically at short elapsed times after a metal is added to the protein [27,29,78]) Ag(I) and Cu(I) bind preferentially first to the β domain, while Cd(II) binds in the α domain. Spectroscopic studies suggest that when either Cd(II) [29] or Cu(I) [27,78] are titrated into dilute solutions of Zn_7-MT the incoming metals bind to both domains on a statistical basis, that is no domain specificity is exhibited initially. At room temperature and above, Cd(II) migrates to the α domain, while Cu(I) migrates to the β domain, thus forming the domain specific, thermodynamically-equilibrated product described first by Winge. We have found no indication in titrations of Zn_7-MT with Cd(II) or Cu(I) of cooperative

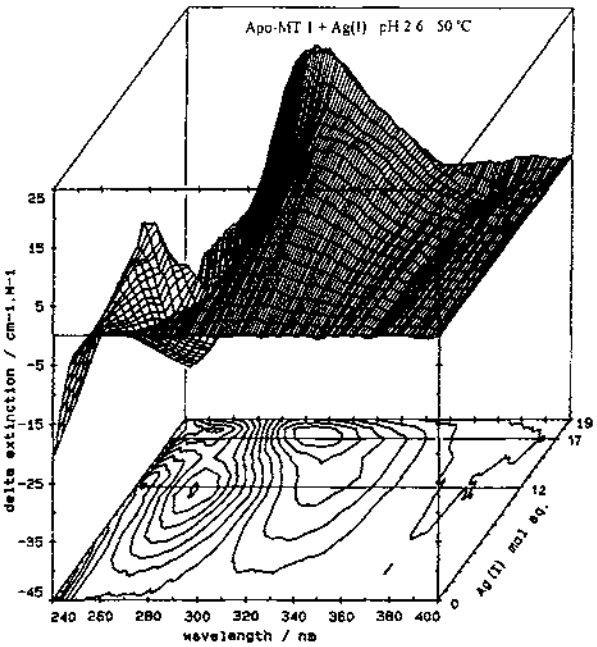

Fig. 13. CD spectra recorded during a titration of rabbit liver apo-MT 2 with Ag(I) at 50 °C and pH 2.6; Ag_{12}-MT 1 forms first, followed by Ag_{17}-MT. Reproduced with permission from Ref. [178].

binding [209]. In this mechanism, metal binding forms a completely filled domain with all available metal rather than distributing the metal more thinly across all available protein molecules. For example, if a cooperative mechanism operated fully when 1 mol eq Cu(I) were added to a solution of Zn_7-MT, the stoichiometric mix of the product would be 1/12 Cu_{12}-MT and 11/12 Zn_7-MT. The spectroscopic signature of this complex following formation by this cooperative mechanism would intensify linearly up to a maximum where 12/12 Cu_{12}-MT formed and all the Zn(II) was displaced. There is a dramatic nonlinearity in the changes observed in the CD spectra that are recorded during Cu(I) titrations of Zn_7-MT, Fig. 5 [78], and apo-MT [210,211]. Similarly, the intensities of the emission spectra recorded during titrations of Cu(I) into solutions of Zn_7-MT at room temperature [27] increase nonlinearly with the molar ratio of Cu(I) to MT, Fig. 7 [27]. These data unambiguously confirm that Cu(I) binding to mammalian Zn-MT does not follow a cooperative mechanism under these conditions. We should qualify this by saying that the conditions used are that the metal salt is added directly to anaerobic solutions of the Zn_7-MT in the spectroscopic cuvette. Determinations of metal location carried out following chemical or biochemical procedures may readily report that complete cluster formation has occurred at less than the saturation point, which is 12 for Cu(I). Under the influence of added EDTA, Stillman and Zelazowski [130] found concentrations of the Cd_4-α fragment remaining following partial digestion of the β peptide by the enzyme subtilisin to be far higher than predicted based on metal

filling calculations. The explanation offered for this effect required the EDTA to act as a carrier for the Cd(II) during the reaction. Otvos et al. [35] reported finding only evidence for Ag_6-MT and Ag_{12}-MT in the HPLC chromatogram following addition of varying molar ratios of Ag(I); concluding that only these two products were made. However, it is possible that interactions on the column allowed the metals to redistribute to form the completely full clusters. No spectroscopic evidence was offered to show that the configuration of the Ag(I) remained the same following elution.

Although several isoforms (and also subisoforms) are known to exist for many sources of metallothionein, few distinctly different binding properties have been reported. The most significant is perhaps the difference in Hg(II) binding between rabbit liver MT 1 and 2, where the CD spectrum for Hg_{18}-MT 1 suggests that the three-dimensional structure does not form [101]. It is not unexpected that metal binding properties should not be the same for the different isoforms if the difference in the amino acid sequence occurs at a key location. Munger et al. [149] speculated that the differences in the CD spectra in the 300–350 nm region for bovine fetal liver Cu, Zn-MT 1 and 2 arise because the amino acid sequences differ mainly in the β terminal.

5.2. *The dynamics of metal binding to metallothionein*

As the structural aspects of the binding site have become established, properties of the metal–thiolate clusters have become important. These properties include, amongst others, the dynamics of the metal binding reaction itself, the equilibrium processes involved in metal substitution reactions, and the kinetics and structural effects of competitive metal chelation by other ligands. NMR studies using Cd-MT suggest that the bound metals are involved in continuous exchange between different sites [34,35], which could account for observation of domain specificity in cases where two different metals are bound to the protein. Similar spectral effects have been reported by our group based on the observation of changes in the CD spectrum following metal binding at temperatures between 5 and 50 °C for a number of different metals [29,78,118,119]. Competition for the metals in the metallothionein binding sites by added ligands is well documented both in vitro [23,24,36,212–214] and in vivo [215,216]. The mobility of Cd(II) and Zn(II) during digestion of the rabbit liver protein to form optimum concentrations of α fragment in the presence of EDTA also illustrates how accessible the bound metals are to competitive ligands [130].

Current studies are now beginning to focus on the details of metal binding in vitro. Particularly, but not exclusively, it is important to determine (i) the dynamics of metal binding, especially the displacement of a bound metal by an incoming metal with a greater binding constant [211,217], (ii) how competitive reactions with added ligands take place [24,213,214], (iii) the extent of metal-induced association between metallothioneins, (iv) the kinetics of both the initial metal binding step and metal transfer reactions between the two domains in the mammalian metallothioneins [24,33–35], and finally, (v) the structures of the metal–thiolate clusters for metals

other than Cd(II) or Zn(II). While Cd(II) and Zn(II) adopt a tetrahedral geometry, with coordination by four thiolates, in both domains of mammalian metallothioneins studied by ^{113}Cd NMR [16,20], X-ray diffraction [6,7], and EXAFS spectroscopy [104], metals such as Cu(I) and Ag(I) bind with trigonal or digonal coordination [62,85,178]. Currently, as described below and illustrated in Table 4, EXAFS is the technique of choice in providing metal–thiolate bond lengths for different metallothioneins, including Cu, Ag, and Hg [218,219].

Overall, the Zn(II), Cd(II), and Cu(I) proteins from both vertebrate and invertebrate organisms, have received the greatest attention spectroscopically [1–5,107]. The spectroscopic properties of a number of other metals bound to metallothionein have been previously described [32] including detailed studies of the binding reactions and spectroscopic properties of Hg(II) [101–104,114,192], Ag(I) [62,118,119], Au(I) [127,220,221], and Co(II) [198].

5.3. *Synthetic peptides*

It is important to point out the increasing role for synthetic chemistry in the study of the properties of metallothioneins. Synthetic peptides are now available with different chain lengths and even substitution of amino acids at key probe locations [45,222].

5.4. *Inorganic metal thiolate complexes*

Metal–thiolate complexes that can model the binding sites in metallothionein play an essential role in providing controls for the spectroscopic techniques. This is particularly important in the use of EXAFS studies where the analysis of the EXAFS signal depends on the correct calibration using known structures of a similar type. Detailed synthetic and spectroscopic data have been reported for a very wide range of metal–thiolate complexes [47,48]. For example, Dance et al. [47] have tabulated synthetic and structural properties for metals in most groups, including a wide range of Cu(I), Ag(I), Cd(II), Zn(II), and Hg(II) thiolate complexes, complexes that offer possible structural models for metallothioneins containing these metals.

6. Spectroscopic properties

The pioneering structural studies were carried out using NMR techniques, for example, [16,20,21,35,62,80–82,122–124,224]. Analysis of ^{113}Cd NMR data for a range of protein samples established that a two-domain cadmium–thiolate cluster structure must exist in native and cadmium-saturated mammalian protein [16]. These ^{113}Cd NMR results were preceded and then followed by detailed experiments with a wide range of techniques, for example ^{1}H NMR, EPR, Raman, CD, MCD, Mossbauer, and spectroscopic analyses based on XAS techniques, EXAFS, XANES, and XPS. Tables 1–4 catalog some of these results.

To date, the most extensive information on the structure and electronic nature of

the metal binding sites has been provided by metal and proton NMR spectroscopy, optical absorption, and CD spectroscopies. Structural information relies heavily on metal–thiolate bond lengths, and essentially the only source of these data for proteins other than the Cd_5Zn_2-MT determined crystallographically [6,7] have been from EXAFS measurements. Considerable EXAFS structural data on copper-containing metallothioneins (both classes 1 and 2) have been reported. The availability of EXAFS data from both the coordinating thiolate sulfur and the bound metal provides information unavailable from other techniques [104,178,223]. One note of caution, the bond lengths determined by the EXAFS technique are averages, and unless large differences exist, the presence of individual sites for a fraction of the metals, can only be recognized from an unusually long or short average bond length, and coordination numbers obtained from analysis of the EXAFS data may represent the coordination of the metal by all ligands and may have wide confidence limits. Essentially, other spectroscopic techniques must be used to determine the coordination-purity of the clusters examined and inorganic models must be used to correlate calculated bond lengths with coordination geometry.

6.1. NMR spectroscopy

NMR spectroscopy has provided the seminal structural information concerning cadmium and zinc binding to mammalian [16,20,80–82,122–124,224], fungal [83], yeast [62,83], and the crustaceans, crab [21] and lobster [19] metallothioneins. The presence in rabbit liver metallothionein of two metal–thiolate domains with structures shown diagrammatically in Fig. 2 was first described by Otvos and Armitage [16] based on their analysis of ^{113}Cd NMR. Later a range of other cadmium-containing proteins were studied including the digested α-fragment of rat liver protein MT [224], crab MT, in which two β-like domains were proposed for the Cd_6-S_{18} MT structure [21], and in the yeast and fungal proteins [62,83] a single domain was inferred.

Clearly, the metal dependent NMR experiments are limited in not being able to provide information about the coupling structure for proteins with non-accessible metals. The ^1H two-dimensional NMR studies have in part filled this gap through measurements of a Cd-containing protein and the analogous Zn-containing protein, for example the study by Messerle et al., on human Zn-MT and Cd-MT [80]. Extension to Cu-containing proteins is problematic, because even though Cu(I) is diamagnetic, the Cu(I) interferes through its quadrupole moment [83] and replacement by Ag(I) is necessary. However, as is evident from the optical spectroscopy of Ag(I), it is not certain that isomorphous replacement can be assumed and that when Cu(I) occupies a trigonal site, that Ag(I) will also occupy that site trigonally [62,118,119,178,180].

6.2. Optical spectroscopy

Optical techniques, such as absorption, CD, MCD and emission, have been used quite generally in the characterization of the metal binding properties of metallothion-

eins. This is because these spectroscopic techniques probe the fine differences between structures formed for different metals (band energies) and for varying metal to protein molar ratios (saturation of signals at specific stoichiometric ratios). Absorption spectra were first used to characterize the pH and metal binding dependencies in native cadmium, zinc–metallothionein isolated by Kagi and Vallee [10]. The highly unusual absence of aromatic residues in all the metallothioneins reported to date, means that transitions of the metal-free protein, or apo-MT, are restricted to wavelengths below about 220 nm (depending on the pH and the ionic strength of the solution). For spectroscopic studies in the 240–800 nm region, all the bands observed are metal-related. We and others have used this property to probe the metal binding site in the protein. If the transitions depend entirely on the presence of both protein and metal, then the optical spectrum provides unique information directly about how the metal ion is bound to the protein. In particular, and most important, we can obtain very precise information about how many metal ions bind in similar environments. In many cases the energies, polarizations, and intensities of transitions are dependent on the nature of the metal (for example, Cd(II), Zn(II), or Cu(I)), the coordinating ligand, and on the symmetry of the ligand coordination. Above 220 nm, the most intense transitions are primarily cysteinyl thiolate to metal charge transfer in nature, that lie between 220 and 400 nm. Much of the published work concerns diamagnetic metals from Groups 11 and 12, with Cd(II) and Zn(II) being the most commonly studied metals. However, metallothioneins formed in vitro with Co(II) [196,203,225], Fe(II) [204–208], Ni(II) [197], and Tc(IV) [226] also exhibit bands in the absorption and magnetic circular dichroism spectra that are assigned to intrametal transitions.

The availability of transitions quite separate in energy from peptide-related transitions means that many optical techniques can provide information about the electronic and geometrical properties of the metallated protein. While the absorption spectrum clearly identifies the presence of new transitions when a metal is added to the metal-free protein, estimates of the stoichiometry of the reaction (protein + nM(II)/(I)→metallated products) can be difficult because of absorption by the metal salt itself, especially below 250 nm.

6.2.1. Circular dichroism spectroscopy

CD spectral data have been reported for protein from a wide variety of sources and almost all metals, Table 2. Some examples include rabbit liver Ag_{12}-MT [118,119], Cu_{12}-MT [78,160,161], Zn_7-MT [29,30], Cd_7-MT [29,30,78], and Hg_7-MT [101–103,114,227], as well as Ag_6-α-MT and Ag-β-MT [118,119], Cd_6-α-MT and Cd_6-β-MT [29,30], Hg_4-α-MT [102], and rat liver Cu_6-α-MT and Cu_6-β-MT [14].

The cadmium, copper, mercury and zinc metallated proteins exhibit a circular dichroism spectrum that extends from below 220 nm to the metal-related charge transfer bands between 280 and 350 nm [29,30,78,101–103,242]. In addition, for transition metals d–d transitions exhibit strong and complex CD spectral envelopes between 400 and 850 nm [32,196–198,204,205]. The CD spectrum for the main group metallothioneins can be interpreted in terms of ligand to metal charge transfer

transitions that take place between the coordinating S_{cys} and the metal. Because these charge transfer transitions take place within a three-dimensional binding site that is formed as the peptide wraps around each metal, there exists the possibility that the binding site itself as a whole may be chiral [32,227]. This has been the key to the analysis of the distinctive CD spectrum observed for Cd_7-MT, Fig. 3 [78]. The set of CD spectra shown in Fig. 3 illustrate the detail provided about both the location of the binding site of the incoming Cd(II), as well as the specific values of the Cd(II) to MT stoichiometric ratios that result in the formation of distinct structures. Very much more complicated spectral changes are observed during titrations of Hg(II) and Cu(I). We can see in Figs. 4, 5 and 8–13, the sensitivity of the CD spectrum towards the formation of three-dimensional structures. In these experiments, the CD intensities saturate at different wavelengths for several metal-to-protein ratios, which we interpret in terms of the formation of a series of structures. For the Hg(II) titration of apo-MT 2 and Zn_7-MT, Figs. 8–12, structures form for Hg:MT = 7, 11 and 18. EXAFS data have recently provided bond lengths and coordination numbers (CN) for the Hg_7-MT 2 (Hg–S = 233 pm and CN = 2) and for the Hg_{18}-MT 2 species (Hg–S = 242 pm, CN = 2, and Hg–Cl = 257 pm) [101–104]. The CD spectra recorded for Cu(I) titrations of Zn_7-MT shown in Figs. 4 and 5, show that the participants in the series of structures that form sequentially as the Cu(I) is added depend on the temperature [78]. At low temperatures (essentially $< 10\,^{\circ}C$) Cu_{12}-MT 2 and Cu_{15}-MT 2 form, at elevated temperatures (for example, at $52\,^{\circ}C$) a new structure, Cu_9Zn_2-MT 2, forms before the Cu_{12}-MT 2 species, and finally Cu_{15}-MT 2 forms. The emission spectral data recorded at a range of temperatures during titrations of Cu(I) into solutions of Zn_7-MT [27] must also be considered in the analysis of these CD spectral data. The emission data show that the Cu_{12}-MT 2 species exhibits the most luminescence, which can be interpreted in terms of exhibiting a structure with least solvent access, Figs. 6 and 7.

6.2.2. Magnetic circular dichroism spectroscopy

In the magnetic circular dichroism (MCD) experiment, a magnetic field aligned with the optical path of a CD spectrometer is used to perturb the ground and excited states of the chromophore. In its simplest form, the MCD spectrum shows either (i) the Faraday A term, a temperature independent, derivative shaped envelope in which the inflection point aligns with the band maximum of the corresponding absorption band, (ii) the Faraday B term, a temperature independent, Gaussian shaped envelope that is centered on the band maximum of the corresponding absorption band or (iii) a Faraday C term, a temperature dependent Gaussian shaped band of either positive or negative sign that resembles the shape of the band envelope in the absorption spectrum. The origin of both the A and C term intensity is a degenerate state. For A terms the excited state must be degenerate, for C terms the ground state must be degenerate. These highly characteristic spectral features uniquely identify the symmetry of the chromophore and allow the corresponding absorption spectrum to be assigned. The Faraday B term arises from mixing between all available and accessible states under the perturbation of the applied magnetic field. B terms are generally much weaker than either A or C terms (at low temperatures) and are not as useful

diagnostically. Like the A term, the B term intensity is independent of temperature. Thus, C terms can be readily distinguished from B terms by measuring the MCD spectrum over a range of temperatures. A very complete description of the theoretical background to MCD spectroscopy has been given by Piepho and Schatz [228] and the application of MCD spectroscopy has been reviewed recently by Hollebone [229]. To date, MCD spectra have been reported for several metallothioneins, including, Cd_7-MT [29,30,32,121,132], Hg_7-MT [102,114], Fe_7-MT [204,205], Co_7-MT [150,197,199,202], and Ni_7-MT [197].

Generally, the MCD spectral information is divided into two regions: charge transfer transitions for all metals and *d–d* transitions for the transition metals. For Cd-MT and Hg-MT, the charge transfer bands are observed between about 240–320 nm and, like the associated CD spectrum, dominate the MCD spectrum, providing specific information on the binding of the metal to the cysteinyl thiolates. Fig. 14 shows a set of MCD and associated CD spectra recorded for a series of individual solutions of apo-MT 2, each with an increasing molar ratio of Hg(II). A distorted derivative signal in the MCD spectrum exhibits a maximum intensity at

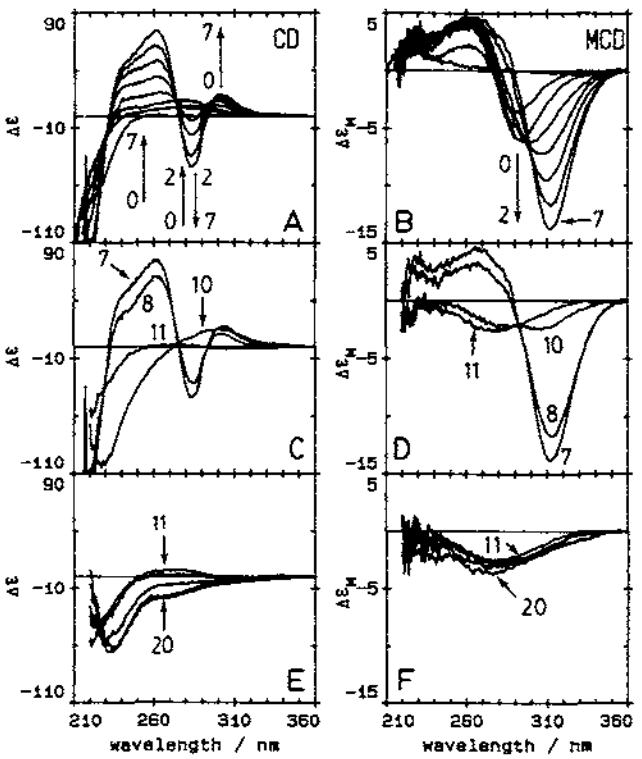

Fig. 14 CD and MCD (at 5.5 T) spectra recorded at pH 7 for separate solutions 10 mM in rabbit liver apo-MT 2, with increasing molar ratios of Hg(II). (A) and (B), for 0–7 Hg(II), (C) and (D), for 7–11 Hg(II), and for (E) and (F), 11, 12, 15, 19, and 20 Hg(II). Note that the MCD signal intensity maximum is near 320 nm. Reproduced with permission from Ref. [102].

the Hg:MT = 7 point. The band maximum in the MCD spectrum is not the same as the CD band maximum, illustrating the differences in the intensity mechanisms involved in the CD and MCD techniques. Comparison between the MCD spectra of $Hg(BAL)_4$ [114] and Hg_7-MT shows that while a distinct A term is apparent in the spectrum of the model compound centered at about 280 nm, the MCD spectral envelope of the protein is very much distorted and does not resemble an A term at all. This suggested that the coordination around the Hg(II) in Hg_7-MT is not symmetrical tetrahedral. Recent XAFS data have been analyzed in terms of two close thiolates at 233 pm, and additional disordered thiolates much further away [104]. For Co-MT, Fe-MT, and Ni-MT, *d–d* transitions in the visible region provide unique information on the spin state of the metal and the coordination geometry. In particular, the MCD spectra of Co-substituted metallothioneins provide unambiguous evidence that the Co(II) are tetrahedrally coordinated by the cysteinyl thiolates [150,197,201]. Similar evidence is found in the MCD spectrum of Ni-MT [197]. Finally, the temperature dependence in the MCD spectrum of Fe-MT reported by Werth and Johnson [205] provides evidence for an S = 2 ground state of the fully loaded $Fe(II)_7$-MT.

6.2.3. Emission spectroscopy

Emission spectra in the 450–750 nm region have been reported for metallothioneins containing Ag(I), Au(I), Cu(I), and Pt(II) [31,32], at both room temperature and cryogenic temperatures,but not for Cd-MT, Hg-MT or Zn-MT. Table 3 summarizes some of these data. d^{10} metals coordinated by thiolates are frequently luminescent at low temperatures as glasses or powders [230]. Figs. 6 and 7 shows the emission spectra recorded for rabbit liver metallothionein for a series of samples with increasing molar ratios of Cu(I). Excitation in the 250–300 nm results in emission intensity in the 500–700 nm region for copper(I), silver(I), and gold(I) metallothioneins [27,31,116,118,121,126–129,135]. The emission is generally characterized by lifetimes of the order a few microseconds [31,121,129]. Although many analogous inorganic compounds luminesce, at present a well-described assignment for the states involved is not available for complexes that do not contain aromatic ligands. We have suggested [31] a scheme that involves excitation into both ligand-to-metal charge transfer states (LMCT) and intrametal states in the 250–300 nm region, followed by intersystem crossing to a purely intrametal triplet state. The unusually large Stoke's shift together with long lived emission that is readily quenched by oxygen, supports an assignment of the emissive state as a triplet in Cu-MT from rabbit liver, for example [27,31]. By extension, the origin of the orange emission from copper-containing metallothioneins from other sources and within a single domain, for example, the yeast metallothioneins, may also be assigned to a triplet, intrametal state.

The most well known emission of the metallothioneins is the orange luminescence observed at room temperature for copper-containing metallothioneins. First reported by Beltramini and Lerch in 1981 [167–170], the subsequent reports suggested that emission intensity in the 550–650 nm region is a general property of copper metallothioneins, see Table 3. As is clear from the data shown in Fig. 7 in which Cu(I) is titrated into a single solution of metallothionein, the emission intensity is entirely

dependent on the molar ratio of Cu(I):Scys. However, in recent work by Green et al. [27], it has been shown that the emission intensity for the two-domain rabbit liver metallothionein actually follows a more complex dependence on the Cu(I):Scys molar ratio than was originally thought. An important trend becomes apparent when the emission intensity profiles for solutions of the protein are plotted as a function of copper loading over a range of temperatures [27,32,121]. At low temperatures (below 10 °C) the quantum yield increases as a function of copper loading roughly linearly from Cu(I):Scys = 1 up to 12, then the intensity collapses steeply towards the 20 Cu(I) point. It is important to point out that if there were no increase in quantum yield as a function of Cu(I) loading, the intensity per Cu(I) would exhibit a flat line from Cu(I):Scys = 1 to 20. We have interpreted the near-20 fold increase in quantum yield to indicate the extreme sensitivity of the emission technique to the environment of the copper–thiolate cluster in the binding site. The excited state is quenched by exposure to the solvent as well as by a variety of quenching agents, for example dioxygen [42]. As Cu(I) is added to either Zn_7-MT or apo-MT, the copper–thiolate cluster structure begins to extend a network of crosslinking bridges that form the three-dimensional structure that makes up the metal binding site. Two such structures are formed for mammalian and crab/lobster copper metallothioneins, one structure for the yeast and fungal proteins. The quite dramatic dependence of the emission intensity on the degree of copper loading provides information on the efficiency of the exclusion of quenching agents and on the degree of overlap of metal based orbitals.

The low temperature data support a model in which between 1 and 12 Cu(I) bind in the two domains. Under these conditions the two domains emit light with an intensity that is approximately dependent on the extent of the domain formation. At high temperatures the data provide information about which domain each copper atom binds to. In a series of papers, Winge and coworkers [125,164,165], reported on the domain specificity of a number of metals that bind to metallothionein. For mammalian metallothioneins, under the conditions used, Cu(I) was observed to bind preferentially to the β domain while cadmium binds preferentially to the α domain. Obtaining dynamic data on the specific metal binding site is difficult, especially for metals as chromophorically silent as Cu(I). However, the emission intensity profile shown as Fig. 7 that was recorded at 40 °C [27] can be interpreted in terms of the site occupied by the incoming Cu(I). In these experiments Cu(I) is added to a single solution of Zn_7-MT. As shown by CD spectral data recorded during Cd(II), Cu(I), Figs. 4 and 5, and Hg(II) titrations of Zn-MT metal binding in metallothioneins is highly temperature dependent. At higher temperatures, here 40 °C, a quite different pattern is observed compared with the data for 10 °C. Significantly, the quantum yield of emission falls as from 1 to 6 Cu(I) are added to the Zn-MT, there then follows a dramatic increase in quantum yield to the 12 Cu(I) point. The interpretation of these and other supporting data, is that the copper–thiolate clusters in the β domain emit far less light than the copper–thiolate clusters in the α domain. At these temperatures, the data support a model in which Cu(I) binds across both domains initially, then migrates to the β domain. At low temperatures the kinetics slow this migration to the point at which only the kinetic product is found and copper–

thiolate structures build in both domains, which results in a linear increase in emission intensity. Finally, a number of compounds will quench the copper emission in rabbit liver metallothionein. Oxygen is a reversible quencher, in the presence of oxygen the emission falls to zero, but the associated CD spectra show that the three-dimensional structure of the Cu-MT has not been disrupted [42]. However, addition of ferricyanide or acrylamide, which also quenches the emission, disrupt the three-dimensional structure of the protein [42].

7. Structural properties

The initial structural characterizations were based on stoichiometric data for cadmium and zinc containing mammalian protein in which seven divalent metal ions were bound to the 20 cysteinyl thiolates (S_{cys}). As described above, the domain structure was first determined by Otvos and Armitage based on ^{113}Cd NMR studies [16]. Winge and Miklossy [165] proposed the 2 domain arrangement for mammalian metallothioneins that was subsequently fully described from X-ray crystallographic [6,7] and ^{1}H NMR studies [20]. The structure of each of the metallothioneins can be described in terms of two general properties. (i) The distribution and orientation in three-dimensional space of each amino acid in the peptide chain, this is in effect the description of the binding site cage as seen from outside the protein. (ii) The connectivities between a specific S_{cys} and one or more of the bound metals and the corresponding coordination geometry around each metal.

Three-dimensional structural parameters that describe the distribution of amino acids and provide a description of the path the peptide chain takes, can be extracted from analysis of ^{1}H NMR data. These data do not provide information on the S_{cys}–metal connectivities except by extension or by using metal–proton interactions. Wuthrich and coworkers have carried out this procedure for Cd-MT [20,80–82,123,124]. The key factor in establishing the internal structure of the binding site, i.e. (ii), is to obtain unambiguous stoichiometric data that relates the number of metals to the number of coordinating S_{cys}. This number essentially controls the possible geometries and the internal structure of the binding site. Spectral studies from my laboratory have shown in several instances that mammalian metallothionein (rabbit liver MT 2a in most of our experiments) binds metals over a continuum of stoichiometric ratios. We have reported on the structural changes that take place when up to 18 Cu(I) bind to Zn_7-MT most recently [78]. While certain ratios may be considered to be *magic numbers*, that is unique metal to sulfur stoichiometries, structures must exist that accommodate all the Cu(I) added together with the remaining Zn(II) atoms. During the titration of Cu(I) into Zn_7-MT, however, well defined Cu-S structures also clearly form at specific stoichiometric ratios, the magic numbers. The existence of these structures is signaled by maxima or saturation points in the spectroscopic data [78].

A major role for synthetic inorganic chemistry has been in providing metal thiolate structures that model the domains in the class I and II proteins [47]. The Cd_4S_{11} and Cd_3S_9 clusters found in the mammalian proteins are readily accounted for by

adamantane-like clusters; both involve tetrahedral coordination of the metal by thiolate ligands [231]. A number of good models are available that provide metal-thiolate bond lengths of the order determined, largely by EXAFS techniques, for Zn_7-MT and Cd_7-MT. For example, see the data of Dean and Vittal [48], and the X-ray structure of the $Zn_4(SR)_{10}$ ion reported by Huang et al. [232], in which the average $Zn–S_{bridging} = 235.8$ pm and $Zn–S_{terminal} = 225.7$ pm. Trigonally coordinated Hg(II), and also Cd(II) and Zn(II), reported by Koch and coworkers [233] might provide the model for the structure of rabbit liver Hg_{11}-MT identified spectroscopically [102]. Much greater variety is found in the structures of Cu(I) and Ag(I) thiolates. Coordination geometries including tetrahedral, trigonal and digonal have been reported, for example for Cu(I) [231,234–236] and Ag(I) [231,237–239]. The formation of chains and cycles based on units of ...RS-Ag-SR-Ag-SR... as determined by Dance and coworkers [240] may provide models for the structure of the binding site in the unusual $Ag_{17/18}$-MT and Hg_{18}-MT identified from spectroscopic studies [101–106,118,119,178]. Together, structural studies of inorganic metal thiolates provide evidence for variable coordination numbers, distorted structures (for example, T-shaped, trigonal coordination), and metal–thiolate bond lengths for each geometry. Recently, Pickering et al. [85] used the availability of so many bond lengths to assign fractions of digonal and trigonal coordination to the Ag(I) and Cu(I) thiolate clusters in Ag-MT and Cu-MT.

7.1. X-ray crystallography

To date, Stout has reported the only structure determined from a crystal [6,7]. The sample was the mixed metal Cd_5Zn_2-MT prepared from rat liver. Significantly, the three-dimensional, space-filling model drawn for Cd_5Zn_2-MT [6,7] showed clearly that deep crevices formed when the peptide chain was wrapped round the two metal–thiolate cores in mammalian metallothionein. The presence of these crevices has been used to account for the variable efficiency of solvent access to the copper–thiolate structures in Cu_n-MT ($n = 1–20$) as indicated by the quantum yield of emission from Cu-MT formed from rabbit liver Zn-MT (and also apo-MT) [27], and as the site of demetallation of Zn-MT by glutathione disulfide [25]. It is possible that these crevices are also the site of interprotein metal exchange. Similar crevices are observed in the structure of Cu_{12}-MT constructed by molecular modeling [78,79].

7.2. X-ray absorption spectroscopy (XAS)

X-ray photoelectron spectra (XPS) using a single element X-ray source have been used to characterize the oxidation state of the bound copper in chicken and rat liver MT [241]. More recently, sulfur L-edge X-ray absorption near-edge structure (XANES) has been used to compare the environments of the coordinating S_{cys} in rabbit liver Zn_7-MT, Cd_7-MT, Hg_7-MT and Hg_{18}-MT [178,223]. Detailed structural information can be inferred from XAS measurements using EXAFS data from the protein and model compounds using both the metals (typically, Zn, Cd, Cu, and Hg) or sulfur as the absorbing atom. While the extracted bond lengths for Zn–S

and Cd–S from model compounds, $[Cd_4(SPh)_{10}]^{2-}$ and $[Zn_4(SPh)_{10}]^{2-}$ closely matched the data from X-ray crystallography and the EXAFS study of Stephan and Hitchcock [242], the XANES data for the proteins were much more complicated [223]. The close similarity of these S_{cys}-based XANES data did show that the environment of the sulfurs in Cd_7-MT and Zn_7-MT must be almost the same as has also been shown more recently in greater detail by ^1H NMR [20,80]. The XANES data for the mercury-containing protein suggested that there was a significant change in the environment of the metal–thiolate clusters in Hg_{18}-MT. The CD spectral data for Hg_{18}-MT [101] are quite unique again suggesting a different environment in this species.

X-ray absorption fine structure (XAFS or EXAFS) data obtained using XAS techniques on synchrotron storage rings offer detailed information on the environment surrounding the absorbing atom. The X-ray energy must be adjusted to match the absorption of a specific edge of the element, for the purposes of studying metallothioneins, low energy X-rays can be used on the K- and L-edges of the sulfur to provide bond lengths and coordination geometries around the coordinating S_{cys} groups [178,223]. Using higher energies, metal edges can be accessed, and XAFS data obtained for each of the bound metals. XAFS data from a wide range of proteins have been reported by Hasnain and coworkers [218], Winge and coworkers [59,61,85,243], and recently from our group [104,178]. These data are summarized in Table 4. Figs. 15 and 16 show data obtained by my laboratory; the raw data in

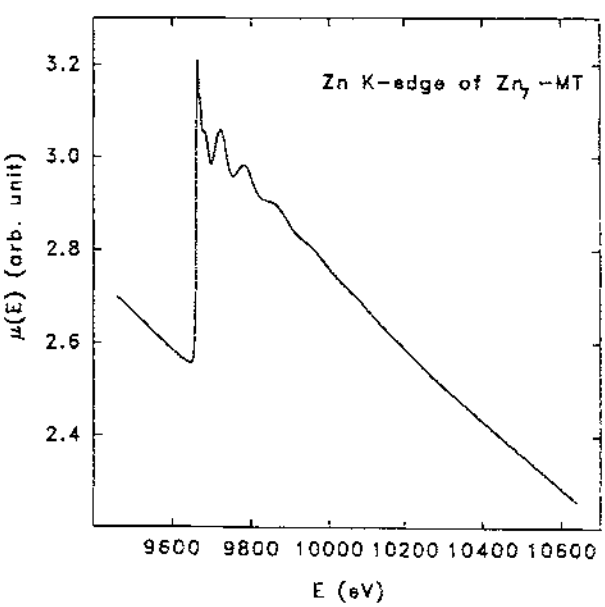

Fig. 15. The experimentally determined data for Zn K-edge absorption recorded for a solid sample of Zn_7-MT 2 at 77 K. Reproduced with permission from Ref. [104].

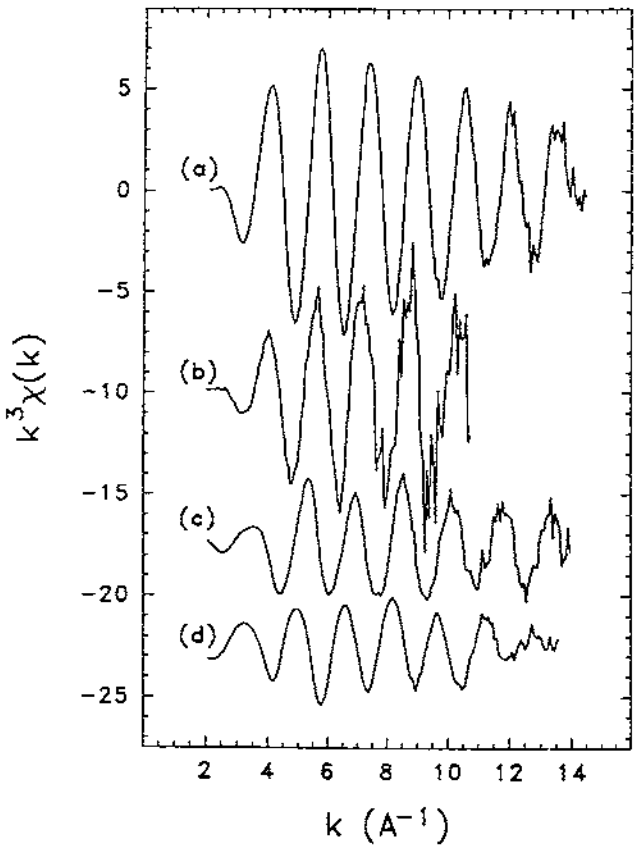

Fig. 16. Metal absorption edge XAFS data for (a) Zn_7-MT 2, (b) Cd_7-MT 2, (c) Hg_7-MT 2, and (d) Hg_{18}-MT 2, plotted as $k^3\chi(k)$ data. Analysis of the first shell with a nonlinear least-squares curve-fitting procedure gave bond lengths as: Zn–S = 234.9 pm; Cd–S = 250.0 pm; Hg–S = 233.0 pm in Hg_7-MT and Hg–S = 241.0 pm in Hg_{18}-MT 2. Reproduced with permission from Ref. [104].

Fig. 15 and the XAFS data for the proteins Zn_7-MT, Cd_7-MT, Hg_7-MT and Hg_{18}-MT 2 in Fig. 16 [104].

Generally, for Zn–MT, the Zn–S bond length of 235 pm closely matches that found for Zn(II) in known inorganic compounds that adopt tetrahedral coordination geometries [47,84]. Similarly for Cd–S in Cd-MT, the 250 pm bond length and CN = 4 reported most recently from the XAFS experiments [104] fits known inorganic structures and also the structure determined by ^{113}Cd NMR [16]. The data for Ag(I), Cu(I), and Hg(II) are not quite as easy to interpret. From sulfur K-edge EXAFS [178,180], we have calculated that the Ag–S bond length in both Ag_{12}-MT 1 and Ag_{17}-MT 1 is approx. 245 ± 3 pm, with the extent of digonal coordination of the Ag(I) by S increasing in the Ag_{17}-MT 1 when compared with the Ag_{12}-MT 1. Sulfur K-edge XAFS data for Zn-MT, Cd-MT, and Ag-MT from rabbit liver [178] suggest that the coordination of the sulfur can be determined from the S K-edge

EXAFS experiment. Considerable data exist for copper-containing metallothioneins, see Table 4. Clearly, from the optical data presented above, the Cu:S_{cys} stoichiometry must be carefully controlled, so also must the temperature at which the protein sample is metallated if metallation is carried out in vitro [27]. Cu–S bond lengths in Cu_{12}-MT from mammalian sources, fungus, and yeast are reported to be approximately 225 pm, a value that is on the short side for some trigonal Cu(I) in model compounds [85]. Recently, Pickering et al. [85] proposed, based on XAFS measurements of Cu-MT from a number of species that the value of the bond length determined in each case represents an average for Cu(I) atoms that adopt either digonal and trigonal geometry in the same domain. So that for pig Cu-MT they propose that 70% of the Cu(I) is trigonal and 30% is digonally coordinated. They propose that in yeast Cu-MT 30% of the Cu(I) is digonally coordinated while in *N. crassa* Cu-MT, 50% is digonally coordinated [85]. While some of the justification for this approach comes from an NMR study of the coordination of Ag(I) in yeast Ag-MT [62], our CD [118,119] and very recent S K-edge EXAFS [178] data suggest that Cu(I) and Ag(I) cannot be considered to adopt isomorphous binding geometries. Rather, Ag(I) is expected to adopt a geometry with greater fraction of digonal coordination than Cu(I). The CD data shown as Fig. 5 suggest that titrations ought to be carried out to determine whether the trigonal/digonal mixture occurs at all molar ratios or just close to 12. Our CD data strongly suggest that at the low concentrations used for the optical experiments, only trigonal Cu(I) forms up to 12 Cu(I), but that a new species with a maximum at 15 Cu(I) might involve both trigonal and digonal coordination [78].

A similar problem has been found for Hg-MT. Results from Hasnain's group give the Hg–S bond lengths as 242 pm and a coordination number of 3 for Hg_7-MT [218]. Analysis of our more recent results based on Hg-L_3-edge XAS measurements [104] on samples for which CD data confirm that just 7 or 18 Hg(II) are bound [101–103] gives average Hg–S bond lengths of 233 pm and coordination number of 1.8(0.5) for Hg_7-MT and 241(1) pm and 1.9(2) for Hg_{18}-MT. In this case, it is essential that the $Hg:_{cys}$ molar ratio be controlled accurately. The analysis of these measurements suggests that in Hg_7-MT 2 Hg(II) does not adopt a purely tetrahedral geometry, rather the Hg(II) adopts a structure with two close S and two distant S, much like many inorganic Hg(II) compounds [84]. In the Hg_{18}-MT 2 the increased precision, and longer bond lengths indicates that a weak feature at 257 pm represents bonding to chloride ion. Earlier studies [101] had shown a dependency of the Hg_{18}-MT 2 structure on chloride ion concentration.

Acknowledgments

I gratefully acknowledge the continuing financial support from NSERC of Canada and the Academic Development Fund at the UWO. The work described from my laboratory was carried out by a number of collaborators, most recently, Drs. Merce Capdevila, Anna Rae Green, De-Tong Jiang, Anthony Presta, and Ziqi Gui, and I gratefully thank them all for their skill, enthusiasm, and imagination in probing the

metal binding properties of metallothionein. I also wish to thank Drs. G.M. Bancroft, P.A.W. Dean, M. Kasrai, and T.K. Sham at the UWO for collaboration on the XAS studies.

References

[1] J.H.R. Kagi and M. Nordberg (eds.), Metallothionein, Birkhauser, Basel, 1979.
[2] J.H.R. Kagi and Y. Kojima (eds.), Metallothionein II, Birkhauser, Basel, 1987.
[3] M.J. Stillman, C.F. Shaw and K.T. Suzuki (eds.), Metallothioneins. Synthesis, Structure and Properties of Metallothioneins, Phytochelatins and Metal-thiolate Complexes, VCH, New York, 1992.
[4] K.T. Suzuki, N. Imura and M. Kimura (eds.), Metallothionein III, Birkhauser, Basel, 1993.
[5] J.F. Riordan and B.L. Vallee (eds.), Metallobiochemistry Part B. Metallothionein and Related Molecules. Methods in Enzymology, Vol. 205, Academic Press, New York, 1991.
[6] A.H. Robbins, D.E. McRee, M. Williamson, S.A. Collett, N.H. Xuong, W.F. Furey, B.C. Wang and C.D. Stout, J. Mol. Biol., 221 (1991) 1269–1293.
[7] A.H. Robbins and C.D. Stout, in M.J. Stillman, C.F. Shaw III, K.T. Suzuki (eds.), Metallothioneins, VCH, New York, 1992, Chap. 3, pp. 31–54.
[8] M. Margoshes and B.L. Vallee, J. Am. Chem. Soc., 79 (1957) 4813–4814.
[9] J.H.R. Kagi and B.L. Vallee, J. Biol. Chem., 235 (1960) 3460–3465.
[10] J.H.R. Kagi and B.L. Vallee, J. Biol. Chem., 236 (1961) 2435–2442.
[11] B.L. Vallee and W. Maret, in K.T. Suzuki, N. Imura and M. Kimura (eds.), Metallothionein III, Birkhauser, Basel, 1993, pp. 1–27.
[12] K. Fuwa, in E.C. Foulkes (ed.), Biological Role of Metallothioneins, Elsevier, New York, 1982, p.1.
[13] X. Yu, M. Wojciechowski and C. Fenselau, Anal. Chem., 65 (1993) 1355–1359.
[14] Y.-J. Li and U. Weser, Inorg. Chem., 31 (1992) 5526–5533.
[15] Y. Le Blanc, A.P. Presta, J. Vienot, M. Siu and M.J. Stillman, submitted.
[16] J.D. Otvos and I.M. Armitage, Proc. Natl. Acad. Sci. USA, 77 (1980) 7094–7098.
[17] U. Weser and H. Rupp, in M. Webb (ed.), The Chemistry, Biochemistry, and Biology of Cadmium, North Holland, Amsterdam, 1979, pp. 267–283.
[18] J.H.R. Kagi, in K.T. Suzuki, N. Imura and M. Kimura (eds.), Metallothionein III, Birkhauser, Basel, 1993, pp. 29–55.
[19] Z. Zhu, E.F. DeRose, G.P. Mullen, D.H. Petering and C.F. Shaw III, Biochem., 33 (1994) 8858–8865.
[20] W. Braun, M. Vasak, A.H. Robbins, C.D. Stout, G. Wagner, J.H.R. Kagi and K. Wuthrich, Proc. Natl. Acad. Sci. USA. 89 (1992) 10124–10128.
[21] J.D. Otvos, R.W. Olafson and I.M. Armitage, J. Biol. Chem., 257 (1982) 2427–2431.
[22] H. Fliss and M. Menard, Arch. Biochem. Biophys., 293 (1992) 195–199.
[23] M.M. Savas, C.F. Shaw III and D.H. Petering, J. Inorg. Biochem., 52 (1993) 235–249.
[24] D.H. Petering, S. Krezoski, P. Chen, A. Pattanaik and C.F. Shaw, in M.J. Stillman, C.F. Shaw and K.T. Suzuki (eds.), Metallothioneins, VCH, New York, 1992, pp. 164–185.
[25] W. Maret, Proc. Natl. Acad. Sci. USA, 91 (1994) 237–241.
[26] Z. Zhu, M. Goodrich, A.A. Isab and C.F. Shaw III, Inorg. Chem., 31 (1992) 1662–1667.
[27] A.R. Green, P.A. Presta, Z. Gasyna and M.J. Stillman, Inorg. Chem., 33 (1994) 4159–4168.
[28] A.M. Da Costa Ferreira, M.R. Ciriolo, L. Marcocci and G. Rotilio, Biochem. J., 292 (1993) 673–676.
[29] M.J. Stillman and A.J. Zelazowski, Biol. Chem., 263 (1988) 6128–6133.
[30] M.J. Stillman, W. Cai and A.J. Zelazowski, Biol. Chem., 262 (1987) 4538–4548.
[31] M.J. Stillman, and Z. Gasyna, in J.F. Riordan and B. L. Vallee (eds.), Methods in Enzymology, Metallobiochemistry part B, Metallothionein and Related Molecules, Academic Press, Chap. 62, 1991, pp. 540–555.
[32] M.J. Stillman, in M.J. Stillman, C.F. Shaw and K.T. Suzuki (eds.), Metallothioneins. Synthesis,

Structure and Properties of Metallothioneins, Phytochelatins and Metal-Thiolate Complexes, VCH, New York, Chap. 4, 1992, pp. 55–127.
[33] D.G. Nettesheim, H.R. Engeseth and J.D. Otvos, Biochem., 24 (1985) 6744–6751.
[34] J.D. Otvos, H.R. Engeseth, D.G. Nettesheim and C.R. Hilt, in J.H.R. Kagi and Y. Kojima (eds.), Metallothionein II, Birkhauser, Basel, 1987, pp. 171–178.
[35] J.D. Otvos, X. Liu, H. Li, G. Shen and M. Basti, in K.T. Suzuki, N. Imura and M. Kimura (eds.), Metallothionein III, Birkhauser, Basel, 1993, pp. 57–74.
[36] T.-Y. Li, A.J. Kraker, C.F. Shaw III and D.H. Petering, Proc. Natl. Acad. Sci. USA, 77 (1980) 6334–6338.
[37] K. Tamai, E.B. Gralla, L.M. Ellerby, J.S. Valentine and D.J. Thiele, Proc. Natl. Acad. Sci. USA, 90 (1993) 8013–8017.
[38] M. Satoh, Y. Kondo, M. Mita, I. Nakagawa, A. Naganuma and N. Imura, Cancer Research, 53 (1993) 4767–4768.
[39] R.V. Parish, Int. Sci. Rev., 17 (1992) 221–228.
[40] K.A. Morton, B.J. Jones, M.-H. Sohn, F. Datz and R.E. Lynch, J. Pharm. Exp. Therapeutics, 267 (1993) 697–702.
[41] C. Simkins, P. Eudaric, C. Torrence and Z. Yang, Life Sci., 53 (1993) 1975–1980.
[42] A.R. Green and M.J. Stillman, Inorg. Chim. Acta, 226 (1994) 275–283.
[43] I. Bremner, in J.H.R. Kagi and Y. Kojima (eds.), Metallothionein II, Birkhauser, Basel, 1987, pp. 81–108.
[44] M. Webb, in J.H.R. Kagi and Y. Kojima (eds.), Metallothionein II, Birkhauser, Basel, 1987, pp. 109–134.
[45] Y. Okada, K. Tanaka, J.-I. Sawada and Y. Kikuchi, in M.J. Stillman, C.F. Shaw III, K.T. Suzuki (eds.), Metallothioneins, VCH, New York, 1992, pp. 195–225.
[46] M. Isobe, Y. Hayashi, K. Imai, C.-W. Nakagawa, D. Uyakul, N. Mutoh and T. Goto, in M.J. Stillman, C.F. Shaw III, K.T. Suzuki (eds.), Metallothioneins, VCH, New York, 1992, pp. 226–256.
[47] I. Dance, K. Fisher and G. Lee, in M.J. Stillman, C.F. Shaw III, K.T. Suzuki (eds.), Metallothioneins, VCH, New York, 1992, pp. 284–345.
[48] P.A.W. Dean and J.J. Vittal, in M.J. Stillman, C.F. Shaw III, K.T. Suzuki (eds.), Metallothioneins, VCH, New York, 1992, pp. 346–386.
[49] M.J. Stillman, P.A. Presta, Z. Gui and D.-T. Jiang, Metal-Based Drugs, 1 (1994) 375–393.
[50] A. Chatterjee and I.B. Maiti, Mol. Cell. Biochem., 108 (1991) 29–38.
[51] H.M. Chan, M. Satoh, R.K. Zalups and M.G. Cherian, Toxicol., 76 (1992) 15–26.
[52] J.W. Bauman, J.Y.P. Liu and C.D. Klassen, Toxicol. Appl. Pharmacol., 110 (1991) 347–354.
[53] K.-S. Min, Y. Terano, S. Onosaka and K. Tanaka, Toxicol. Appl. Pharmacol., 111 (1991) 152–162.
[54] M. Greger, E. Brammer, S. Lindberg, G. Larsson and J. Idestam-Almquist, J. Exp. Botany, 42 (1991) 729–737.
[55] D.R. Winge, R. Premakumar and K.V. Rajogopalan, Arch. Biochem. Biophys., 170 (1975) 242–252.
[56] M.G. Cherian and H.M. Chan, in K.T. Suzuki, N. Imura and M. Kimura (eds.), Metallothionein III, Birkhauser, Basel, 1993, pp. 87–109.
[57] D.H. Hamer, in K.T. Suzuki, N. Imura and M. Kimura (eds.), Metallothionein III, Birkhauser, Basel, 1993, pp. 347–350.
[58] L. Gedamu, R. Foster, N. Jahroudi, S. Samson, N. Shworak and M. Zafarullah, in K.T. Suzuki, N. Imura and M. Kimura (eds.), Metallothionein III, Birkhauser, Basel, 1993, pp. 363–380.
[59] D.R. Winge and C.T. Dameron, in K.T. Suzuki, N. Imura and M. Kimura (eds.), Metallothionein III, Birkhauser, Basel, 1993, pp. 381–397.
[60] Y. Kojima, in J.F. Riordan and B.L. Vallee (eds.), Methods in Enzymology, Vol. 205, Academic Press, New York, 1991, pp. 8–10.
[61] G.N. George, J. Byrd and D.R. Winge, J. Biol. Chem., 263 (1988) 8199–8203.
[62] S.S. Narula, R.K. Mehra, D.R. Winge and I.M. Armitage, J. Am. Chem. Soc., 113 (1991) 9354–9358.
[63] W.E. Rauser, in K.T. Suzuki, N. Imura and M. Kimura (eds.), Metallothionein III, Birkhauser, Basel, 1993, pp. 223–242.

[64] N.J. Robinson, A.M. Tommey, C. Kuske and P.J. Jackson, Biochem. J., 295 (1993) 1–10.
[65] D.R. Winge, C.T. Dameron and R.K. Mehra, in M.J. Stillman, C.F. Shaw III, K.T. Suzuki (eds.), Metallothioneins, VCH, New York, 1992, pp. 257–270.
[66] Y. Hayashi and D.R. Winge, in M.J. Stillman, C.F. Shaw III, K.T. Suzuki (eds.), Metallothioneins, VCH, New York, 1992, pp. 271–283.
[67] I. Bremner, in K.T. Suzuki, N. Imura and M. Kimura (eds.), Metallothionein III, Birkhauser, Basel, 1993, pp. 111–124.
[68] G. Roesijadi, in K.T. Suzuki, N. Imura and M. Kimura (eds.), Metallothionein III, Birkhauser, Basel, 1993, pp. 141–158.
[69] M. Nordberg and G.F. Nordberg, in J.H.R. Kagi and Y. Kojima (eds.), Metallothionein II, Birkhauser, Basel, 1987, pp. 669–675.
[70] W. Stremmel, K.-W. Meyerrose, C. Niederau, H. Hefter, Kreuzpainter and G. Strohmeyer, Ann. Int. Medicine, 115 (1991) 720–726.
[71] P.E. Hunziker and I. Sternlieb, Eur. J. Clin. Inv., 21 (1991) 466–471.
[72] M.P. Waalkes, in K.T. Suzuki, N. Imura and M. Kimura (eds.), Metallothionein III, Birkhauser, Basel, 1993, pp. 243–253.
[73] A. Naganuma, M. Satoh and N. Imura, in K.T. Suzuki, N. Imura and M. Kimura (eds.), Metallothionein III, Birkhauser, Basel, 1993, pp. 255–268.
[74] N. Saijo, K. Miura and K. Kasahara, in K.T. Suzuki, N. Imura and M. Kimura (eds.), Metallothionein III, Birkhauser, Basel, 1993, pp. 279–291.
[75] D.H. Petering, A. Quesada, M. Dughish, S. Krull, T. Gan, D. Lemkuil, A. Pattanaik, R.W. Brynes, M. Savas, H. Whelan and C.F. Shaw, in K.T. Suzuki, N. Imura and M. Kimura (eds.), Metallothionein III, Birkhauser, Basel, 1993, pp. 329–346.
[76] A. Pattanaik, C.F.III Shaw, D.H. Petering, J. Garvey and A.J., Kraker, J. Inorg. Biochem., 54 (1994) 91–105.
[77] K.T. Suzuki in, M.J. Stillman, C.F. Shaw and K.T. Suzuki, (eds.) Metallothioneins, V.C.H. Publishers, New York 1992, pp. 14–30).
[78] P.A. Presta, A.R. Green, A.J. Zelazowski and M.J. Stillman, Eur. J. Biochem., 227 (1995) 226–240.
[79] P.A. Presta, H. Zinnen, D. Galagher and M.J. Stillman, submitted.
[80] B.A. Messerle, A. Schaffer, M. Vasak, J.H.R. Kagi, and K.J. Wuthrich, Mol. Biol. 225 (1992) 433–443.
[81] M. Vasak, E. Worgotter, G. Wagner, J.H.R. Kagi, and K. Wuthrich, J. Mol. Biol., 196 (1987) 711–719.
[82] E. Worgotter, G. Wagner, M. Vasak, J.H.R. Kagi, and K. Wuthrich, Eur. J. Biochem., 167 (1987) 457–466.
[83] J.A. Malikayil, K. Lerch and I.M. Armitage, Biochem., 28 (1989) 2991–2995.
[84] A.J. Carty and S.F. Malone in, J.O. Nriagu (ed.), The Biogeochemistry of Hg in the Environment, Elsevier, Amsterdam 1979, pp 433–479.
[85] I.J. Pickering, G.N. George, C.T. Dameron, B. Kurz, D.R. Winge and I.G. Dance, J. Am. Chem. Soc., 115 (1993) 9498–9505.
[86] E.C Foulkes (ed.), Biological Roles of Metallothionein, Elsevier, New York (1982).
[87] M. Webb (ed.), The Chemistry, Biochemistry, and Biology of Cadmium, Elsevier, North Holland (1979).
[88] J.H. Mennear (ed.), Cadmium Toxicity, Marcel Dekker, New York (1979).
[89] K. Robards and P. Worsfold, Analyst, 116 (1991) 549.
[90] C.G. Elinder, M. Nordberg, B. Palm, L. Bjorck and L. Jonsson, in J.H.R. Kagi and Y. Kojima (eds.), Metallothionein II, Birkhauser Verlag, Basel (1987), p. 677–680.
[91] T. Kido, K.A. Shaikh, H. Kito, R. Honda, and K. Nogawa, Toxicology, 66 (1991) 271–278.
[92] K. Iwata, H. Saito, M. Moriyama, A. Nakano, Tohoku J. Exp. Med., 164 (1991) 93–102.
[93] H.-J. Pesch, T. Kraus, K. Biermann, and B. Krapp, Fresenius J. Anal. Chem., 343 (1992) 150–151.
[94] T. Kjellstrom, in Proc. 1st Int. Cadmium Conference, Metal Bulletin Ltd., London 1977, pp 224 – 231.
[95] N.O. Narty, J.V. Frei and M.G. Cherian, Lab. Investigation, 57 (1987) 397–401.
[96] T. Sone, K. Yamaoka, Y. Minami and H. Tsunoo, J. Biol. Chem., 262 (1987) 5878–5885.

[97] A. McQuaid and J. Mason, J. Inorg. Biochem., 41 (1990) 87–92.
[98] J.C. Yarze, P. Martin, S.J. Munoz and L.S. Friedman, Amer. J. Med., 92 (1992) 643–654.
[99] N. Shiraishi, T. Taguchi, and H. Kinebuchi, Toxicol. App. Pharm., 110 (1991) 89–96.
[100] G.J. Brewer and V. Yuzbasiyan-Gurkan, Medecine, 71 (1992) 139–164.
[101] W. Lu, A.J. Zelazowski, and M.J. Stillman, Inorg. Chem., 32 (1993) 919–926.
[102] W. Lu and M.J. Stillman, J. Am. Chem. Soc., 115 (1993) 291 -3299.
[103] W. Lu and M.J. Stillman, J. Am. Chem. Soc., 110 (1988) 7872–7873.
[104] D.T. Jiang, S.M. Heald, T.K. Sham and M.J. Stillman, J. Am. Chem. Soc., 116 (1994) 11004–11013.
[105] C. Cizewski, P. Lapinskas and X.F. Liu in, K.D. Karlin and Z. Tyeklar (eds.), Bioinorganic Chemistry of Copper, Chapman and Hall, New York, 1993, pp 124–131.
[106] C.F. Wright, D.H. Hamer and K. McKenney, J. Biol. Chem., 263 (1988) 1570–1574.
[107] D.R. Winge in, B.L. Vallee and J.F. Riordan, (eds.), Methods in Enzymology, Metallobiochemistry part B, Metallothionein and Related Molecules, Academic Press, (1991) vol. 205, pp 458–469.
[108] M.A. Dunn, M.H. Green and R.M. Leach, Am. J. Physiol., 261 (1991) E115–E125.
[109] J.K. Piotrowski, W. Bolanowska and A. Sapota, Acta Biochem. Pol., 20 (1973) 207.
[110] J.A. Szymanska and A.J. Zelazowski, Env. Res., 19 (1979) 121–126 .
[111] H.V. Aposhian and D.C. Bruce, Rad. Res. 126 (1991) 379.
[112] E.M. Mogilnicka and M. Webb, J. App. Tox., 1 (1981) 288.
[113] Y. Kondo, M. Satoh, N. Imura and M. Akimoto, Cancer Chemother. Pharmacol., 29 (1991) 19–23.
[114] M.J. Stillman, A.Y.C. Law and J.A. Szymanska, in S.S. Brown and J. Savory, (eds.), Chemical Toxicology and Clinical Chemistry of Metals, Harcourt Brace, London 1983, pp 271–274.
[115] A.J. Zelazowski, J.A. Szymanska, A.Y.C. Law and M.J. Stillman, J. Biol. Chem., 259 (1984) 12960–12963.
[116] M.J. Stillman, J.A Szymanska, Biophysical Chemistry, 19 (1984) 163–169.
[117] J.A. Szymanska and M.J. Stillman, Biochem. Biophys. Res. Commun., 108 (1982) 919–925.
[118] A.J. Zelazowski, Z. Gasyna, M.J. Stillman, J. Biol. Chem., 264 (1989) 17091–17099.
[119] A.J. Zelazowski, and M.J. Stillman, Inorg. Chem., 31 (1992) 3363–3370.
[120] P.E. Hunziker in, J.F. Riordan and B.L. Vallee, (eds.), Metallobiochemistry Part B. Metallothionein and Related Molecules. Methods in Enzymology, vol. 205, Academic Press, New York (1991) pp 451–452.
[121] M.J. Stillman, A.Y.C Law, W. Cai, and A.J. Zelazowski, in J.H.R. Kagi and M. Nordberg (eds.), Metallothionein, Birkhauser Verlag, Basel, 1979, pp 203–211.
[122] J.D. Otvos, H.R. Engeseth and S. Wehrli, Biochem., 24 (1985) 6735– 6739.
[123] D. Neuhaus, G. Wagner, M. Vasak, J.H.R. Kagi and K. Wuthrich, Eur. J. Biochem., 151 (1985) 257–273.
[124] G. Wagner, D. Neuhaus, E. Worgotter, M. Vasak, J.H.R. Kagi and K. Wuthrich, Eur. J. Biochem., 157 (1986) 275–289.
[125] K.B. Nielson and D.R. Winge, J. Biol. Chem., 260 (1985) 8698–8701
[126] M.J. Stillman, Z. Gasyna and A.J. Zelazowski, FEBS Letters, 257 (1989) 283–286.
[127] M.J. Stillman, A.J. Zelazowski, J. Szymanska and Z. Gasyna, Inorg. Chim. Acta, 161 (1989) 275–279
[128] M.J. Stillman, A.J. Zelazowski, and Z. Gasyna, FEBS Letters, 240 (1988) 159–162.
[129] Z. Gasyna, A.J. Zelazowski, A.R. Green, E. Ough, and M.J. Stillman, Inorg. Chim. Acta, 153 (1988) 115–118.
[130] M.J. Stillman, and A.G. Zelazowski, Biochemical Journal, 262 (1989) 181–188.
[131] W. Cai, and M.J. Stillman, Inorg. Chim. Acta, 152 (1988) 111–115.
[132] M.J. Stillman, A.Y.C. Law, E.M.K. Lui, and M.G. Cherian, Inorg. Chim. Acta, 124 (1986) 39–45.
[133] A.Y.C. Law, and M.J. Stillman, Biochem. Biophys. Res. Comm., 121 (1984) 1006–1013.
[134] A.Y.C. Law, M.G. Cherian, and M.J. Stillman, Biochim. Biophys. Acta., 784 (1984) 53–61.
[135] J.A. Szymanska, A.J. Zelazowski, and M.J. Stillman, 115 (1983) 167–173.
[136] P.A.W. Dean, A.Y.C. Law, J.A. Szymanska, and M.J. Stillman, Inorg. Chim. Acta., 78 (1983) 275–279.
[137] A.Y.C. Law, and M.J. Stillman, Biochem. Biophys. Res. Commun. 102 (1981) 397–402.
[138] G.K. Carson, P.A.W. Dean, and M.J. Stillman, Inorg. Chim. Acta., 56 (1981) 59–71.
[139] A.Y.C. Law, and M.J. Stillman, Biochem. Biophys. Res. Commun., 94 (1980) 138–143.

[140] Biological Roles of Copper, CIBA Foundation, vol. 79 London, (1980).
[141] I. Bremner, J. Nutr., 117 (1987) 19–29.
[142] W.E.N.D. Evering, S. Haywood, I. Bremner, and J. Trafford, Chem. Biol. Interactions, 78 (1991) 283–295.
[143] I. Bremner, and R.B. Marshall, Br. J. Nutr. 32 (1974) 293–300.
[144] R. Premakumar, D.R. Winge, R.D. Wiley, and K.V. Rajagopalan, Arch. Biochem. Biophys., 170 (1975) 278–288.
[145] R. Premakumar, D.R. Winge, R.D. Wiley, and K.V. Rajagopalan, Arch. Biochem. Biophys., 170 (1975) 267–277;
[146] W.E. Rauser, and N.R. Curvetto, Nature, 287 (1980) 563–564
[147] T.R. Butt, and D.J. Ecker, Microbiol. Rev., 51 (1987) 351–364.
[148] M. Brouwer, D.R. Winge, and W.R. Gray, J. Inorg. Biochem., 35 (1989) 289–303.
[149] K. Munger, U.A. Germann, M. Beltramini, D. Niedermann, G. Baitella-Eberle, J.H.R. Kagi, and K. Lerch, J. Biol. Chem., 260 (1985)10032–10038.
[150] J. Overnell, M. Good, and M. Vasak, Eur. J. Biochem., 172 (1988) 171–177.
[151] D.W. Engel, and M. Brouwer, Biol. Bull., 180 (1991) 447.
[152] M. Brouwer, and T. Brouwer-Hoexum, Arch. Biochem. Biophys., 290 (1991) 207–213.
[153] D.R. Winge, B.L. Geller, J. Garvey, Arch. Biochem. Biophys., 208 (1981) 160–166
[154] M.J. Stillman, and J.A. Szymanska, Biophys. Chem., 19 (1984) 163–169.
[155] D.H. Hamer, D.J. Thiele, and T.T. Lemon, Science, 228 (1985) 685–690.
[156] D.J. Eckert, T.R. Butt, E.J. Sternberg, M.P. Neepert, C. Debouck, J.A. Gorman, and S.T. Crooke, J. Biol. Chem., 261 (1986) 16895–16900
[157] A.R. Thrower, J. Byrd, E.B. Tarbett, R.R. Mehra, D.H. Hamer, and D.R. Winge, J. Biol. Chem., 263 (1988)7037–7042
[158] C.T. Dameron, G.N. George, P. Arnold, V. Santhanagopalan, and D.R. Winge, Biochemistry, 32 (1993) 7294–7301
[159] B.L. Geller, and D.R. Winge, Arch. Biochem. Biophys., 213 (1982) 109–117.
[160] H-J. Hartmann, and U. Weser, Biochim. Biophys. Acta, 491 (1977) 211–222.
[161] U. Weser, H-J. Hartman, A. Fretdorff, and G-J. Strobel, Biochim. Biophys. Acta, 493 (1977) 465–477
[162] D.R. Winge, R. Premakumar, R.D. Wiley, and K.V. Rajagopalan, Arch. Biochem. Biophys., 170 (1975) 253–266
[163] D.R. Winge, in J.H.R. Kagi, and Y. Kojima, (eds.) Metallothionein II, Birshauser Verlag, Basel 1987, pp 213–218.
[164] K.B. Nielson, and D.R. Winge, J. Biol. Chem., 258 (1983) 13063–13069.
[165] D.R. Winge, and K.-A. Miklossy, J. Biol. Chem., 257 (1982) 3471–3476.
[166] K. Lerch, Nature, 284 (1980) 368–370.
[167] M. Beltramini, and M. Lerch, FEBS Letters, 127 (1981) 201–203.
[168] M. Beltramini, and M. Lerch, FEBS Letters, 142 (1982) 219–222.
[169] M. Beltramini, M. Beltramini, and M. Lerch, Biochemistry, 22 (1983) 2041–2048;
[170] M. Beltramini, K. Munger, U.A. Germann, and K. Lerch, in Metallothionein, J.H.R. Kagi, and M. Nordberg, eds., Birkhauser Verlag, Basel 1979, pp 237–241.
[171] J. Byrd, R.M. Berger, D.R. McMillin, C.F. Wright, D. Hamer, and D.R. Winge, J. Biol. Chem., 263 (1988) 6688–6694.
[172] M. Beltramini, G.M. Giacometti, B. Salvato, G. Giacometti, K. Munger, and K. Lerch, Biochem. J., 260 (1989) 189–193.
[173] D.L. Pountney, I. Schauwecker, J. Zarn, and M. Vasak, Biochemistry, 33 (1994) 9699–9705
[174] K. Felix, H-J. Hartmann, and U. Weser, Biol. Metals, 2 (1989) 50–54.
[175] A.P. Presta, and M.J. Stillman, submitted.
[176] A.P. Presta, and M.J. Stillman, Chirality, 6 (1994) 521–530.
[177] M. Vasak, in J.F. Riordan and B.L. Vallee (eds.), Methods in Enzymology, Metallobiochemistry part B, Metallothionein and Related Molecules, Academic Press, (1991) vol. 205, pp 41–44.
[178] Z. Gui, A.R. Green, M. Kasrai, B. Yang, X. Feng, G.M. Bancroft, and M.J. Stillman, (1995) submitted.
[179] K.T. Suzuki, K. Yamamoto, S. Kanno, Y. Aoki, and N. Takeichi, Toxicol. 83 (1993) 149–158.

[180] T.D. Jiang, Z. Gui, S.M. Heald, T.K. Sham, and M.J. Stillman, Proceedings of the 8th International Conference on XAFS, Berlin, Germany (1944).
[181] T. Suzuki, N. Imura, and T.W. Clarkson (eds.), Advances in Mercury Toxicity Plenum, New York (1991),
[182] M.W. Miller and T.W. Clarkson, (eds.) Mercury, Mercurials, and Mercaptans. Thomas, Springfield, USA, (1973),
[183] C.A. McAuliffe, (ed.)The Chemistry of Mercury, McMillan, Toronto (1977).
[184] W. Levason, and C.A. McAuliffe, in C.A. McAuliffe (ed.) The Chemistry of Mercury, McMillan, Toronto 1977, pp 60–108.
[185] J.G. Wright, H-T. Tsang, J.E. Penner-Hahn, and T.V. O'Halloran, J. Am. Chem. Soc., 112 (1990) 2434-2435.
[186] D.R. Rennex, R.T.Cummings, M. Pickett, C.T. Walsh, and M. Bradley, Biochemistry, 32 (1993) 7475–7478.
[187] M. Jakubowski, J. Piotrowski, and B. Trojanowska, Toxicol. Appl. Pharmacol. 16 (1970) 743–753.
[188] J.M. Wisniewska, B. Trojanowska, J. Piotrowski, and M. Jakubowski, Toxicol. Appl. Pharmacol. 16 (1970) 754–763.
[189] M. Nordberg, B. Trojanowska, G.F. Nordberg, Environ. Physiol. Biochem., 4 (1974) 149–158
[190] A.J. Zelazowski, and J.K. Piotrowski, Biochim. Biophys. Acta, 625 (1980) 89–99.
[191] R.K. Zalups, and M.G. Cherian, Toxicology, 71 (1992) 103–117.
[192] B.A. Johnson, and I.M. Armitage, Inorg. Chem., 26 (1987) 3139–3145.
[193] C.K. Jorgensen, Prog. Inorg. Chem., 12 (1970) 101–158.
[194] M. Vasak, J.H.R. Kagi, and H.A.O. Hill, Biochemistry, 20 (1981) 2852–2856
[195] M. Frey, G. Wagner, M. Vasak, O. Sorensen, D. Neuhaus, E. Worgotter, J.H.R. Kagi, R.R. Ernst, and K. Wuthrich, J. Am. Chem. Soc. 107 (1985) 6847-6851.
[196] M. Vasak, J. Am. Chem. Soc., 102 (1980) 3953–3954.
[197] M. Vasak, J.H.R. Kagi, B. Holmquist, and B.L. Vallee, Biochemistry, 20 (1981) 6659–6664.
[198] M. Vasak, and J.H.R. Kagi, Proc. Natl. Acad. Sci. U.S.A., 78 (1981) 6709–6713.
[199] M. Good, and M. Vasak, Biochemistry, 25 (1986) 3328–3334.
[200] I. Bertini, C. Luchinat, L. Messori, M. Vasak, J. Am. Chem. Soc., 111 (1989) 7296–7300.
[201] D.L. Poutney, and M. Vasak, Eur. J. Biochem., 209 (1992) 335–341.
[202] D. Rakshit, and M. Vasak, J. Biol. Chem., 267 (1992) 235–238.
[203] I. Bertini, C. Luchinat, L. Messori, and M. Vasak, Eur. J. Biochem., 211 (1993), 235–240.
[204] M. Good, and M. Vasak, Biochem. 25 (1986) 8353–8356.
[205] M.T. Werth, and M.K. Johnson, Biochem. 28 (1989) 3982–3988.
[206] X. Ding, E. Bill, M. Good, A.X. Trautwein, and M. Vasak, Eur. J. Biochem. 171 (1988) 711–714
[207] X. Ding, C. Butzlaff, E. Bill, D.L. Pountney, G. Henkel, H. Winkler, M. Vasak, and A.X. Trautwein, Eur. J. Biochem., 220 (1994) 827–837.
[208] X. Ding, E. Bill, A.X. Trautwein, H-J. Hartmann, and U. Weser, Eur. J. Biochem., 223 (1994) 841–845.
[209] J. Byrd, and D.R. Winge, Arch. Biochem. Biophys., 250 (1986) 233–237.
[210] P.A. Presta, and M.J. Stillman, submitted.
[211] A.R. Green, P.A. Presta, and M.J. Stillman, submitted.
[212] J.K. Nicholson, P.J. Sadler, and M. Vasak, in J.H.R. Kagi, and Y. Kojima, (eds.) Metallothionein II, Birkhauser Verlag, Basel 1987, pp 191–201.
[213] T.Y. Li, D.T. Minkel, C.F. III Shaw, and D.H. Petering, Biochem. J., 193 (1981) 441–446.
[214] C.F. Shaw, III, M.M. Savas, and D.H. Petering, in J.F. Riordan, and B.L. Vallee, (eds.) Metallobiochemistry Part B. Metallothionein and Related Molecules. Methods in Enzymology, vol. 205, Academic Press, New York (1991) 205, pp 401–414.
[215] M.G. Cherian, P.K. Singh, M.A. Basinger, and S.G. Jones, Toxicol. Appl. Pharmacol., 110 (1991) 241.
[216] M.G. Cherian, Nature, 287 (1980) 871.
[217] A.R. Green, and M.J. Stillman, submitted.
[218] S.S. Hasnain, Topics in Current Chemistry, 147 (1988) 73–93.
[219] C.D. Garner, Adv. in Inorganic Chemistry, 36 (1991) 303–339.

[220] C.F. Shaw, III, D.H. Petering, J.E. Laib, M.M. Savas, and K. Melnick, in J.F. Riordan, and B.L. Vallee, (eds.) Metallobiochemistry Part B. Metallothionein and Related Molecules. Methods in Enzymology, vol. 205, Academic Press, NewYork (1991) 205, pp 469–475.
[221] C.F. Shaw, III and M.M. Savas, in M.J. Stillman, C.F. Shaw, and K.T. Suzuki, eds. Metallothioneins, V.C.H. Publishers, New York 1992, pp 144–163.
[222] S. Matsumoto, S. Nakayama, Y. Nishiyama, Y. Okada, K-S. Min, S. Onosaka, and K. Tanaka, Chem. Pharm. Bull., 40 (1992) 2694–2700.
[223] W. Lu, M. Kasrai, K.H. Tan, G.M. Bancroft, and M.J. Stillman, Inorg. Chem., 29 (1990) 2561–2563.
[224] Y. Boulanger, I.M. Armitage, K.A. Miklossy, and D.R. Winge, J. Biol. Chem., 257 (1982) 13717–13719.
[225] M. Vasak, J. Overnell, and M. Good, in J.H.R. Kagi, and Y. Kojima, eds. Metallothionein II, Birkhauser Verlag, Basel 1987, pp 179–189.
[226] M.M. Morelock, and G.L. Tolman, in J.H.R. Kagi, and Y. Kojima, eds. Metallothionein II, Birkhauser Verlag, Basel 1987, pp 247–253.
[227] H. Willner, W.R. Bernhard, and J.H.R. Kagi, in M.J. Stillman, C.F. Shaw, and K.T. Suzuki, (eds.) Metallothioneins V.C.H. Publishers, New York 1992, pp 128–143.
[228] S.B. Piepho, and P.N. Schatz, in Group Theory in Spectroscopy: With Applications to MCD, Wiley, New York, 1983.
[229] B.R. Hollebone, Spectrochimica Acta Rev., 15 (1993) 493–526.
[230] J.H. Anglin, W.H. Batten, A.I. Raz, and R.M. Sayre, Photochem. Photobiol., 13 (1971) 279–281.
[231] E. Bloch, M. Gernon, H. Kang, G. Ofori-Okai, and J. Zubieta, Inorg. Chem., 28 (1989) 1263–1271.
[232] Z-X. Huang, H-Y. Hu, W-Q. Gu, and G. Wu, J. Inorg. Biochem., 54 (1994) 147–155.
[233] E.S. Gruff, and S.A. Koch, J. Am. Chem. Soc., 112 (1990) 1245–1247.
[234] I.G. Dance, Aust. J. Chem., 31 (1978) 2195–2206.
[235] I.G. Dance, G.A. Bowmaker, G.R. Clark, and J.K. Seadon, Polyhedron, 2 (1983) 1031–1043.
[236] E. Block, H. Kang, G. Ofori-Okai, and J. Zubieta, Inorg. Chim. Acta, 167 (1990) 147–148.
[237] K. Tang, M. Aslam, E. Block, T. Nicholson, and J. Zubieta, Inorg. Chem., 26 (1987) 1488–1497.
[238] I.G. Dance, L.J. Fitzpatrick, and M.L. Scudder, Inorg. Chem., 23 (1984) 2276–2281.
[239] I.G. Dance, Inorg. Chem., 20 (1981) 1487–1492.
[240] I.G. Dance, L.J. Fitzpatrick, D.C. Craig, and M.L. Scudder, Inorg. Chem., 28 (1989) 1853–1861.
[241] G. Sokolowski, W. Pilz, and U. Weser, FEBS Letters, 48 (1974) 222–225.
[242] D.W. Stephan, and A.P. Hitchcock, Inorg. Chim. Acta, 136, (1987) L1–L5.
[243] G.N. George, D.R. Winge, C.D. Stout, and S.P.J. Cramer, Inorg. Biochem., 27 (1986) 213–220.
[244] H. Willner, M. Vasak, and J.H.R. Kagi, Biochem., 26 (1987) 6287–6292.
[245] M.M. Morelock, T.A. Cormier, and G.L. Tolman, Inorg. Chem., 27 (1988) 3137.
[246] W. Bernhard, M. Good, M. Vasak, and J.H.R. Kagi, Inorg. Chim. Acta, 79 (1983) 154.
[247] M.J. Cismowski, and P.C. Huang, Biochem., 30 (1991) 6626–6632.
[248] F.J. Kull, M.F. Reed, T.E. Elgren, T.L. Ciardelli, and D.E. Wilcox, J. Am. Chem. Soc., 112 (1990) 2291–2298.
[249] J. Pande, C. Pande, D. Gilg, M. Vasak, R. Callender, and J.H.R. Kagi, Biochem., 25 (1986) 5526–5532.
[250] T. Elgren, and D.E. Wilcox, Biochem. Biophys. Res. Commun., 163 (1989) 1093–1099.
[251] I. Bertini, C. Luchinat, L. Messori, and M. Vasak, J. Am. Chem. Soc., 111 (1989) 7300–7303.
[252] A. Arseniev, P. Schultze, E. Worgotter, W. Braun, G. Wagner, M. Vasak, J.H.R. Kagi, and K.J. Wuthrich, Mol. Biol., 201 (1988) 637.
[253] I.L. Abrahams, I. Bremner, G.P. Diakun, C.D. Garner, S.S. Hasnain, I. Ross, and M. Vasak, Biochem. J., 236 (1986) 585–589.
[254] T.A. Smith, K. Lerch, and K.O. Hodgson, Inorg. Chem., 25 (1986) 4677–4680.
[255] K.H. Nakagawa, C. Inouye, B. Hedman, M. Karin, T.D. Tullius, and K.O. Hodgson, J. Am. Chem. Soc., 113 (1991) 3621–3623.
[256] H. Strasdeit, A. Duhme, R. Kneer, M.H. Zenk, C. Hermes, and H. Nolting, J. Chem. Soc. Chem. Commun., (1991) 1129–1130.

[257] P. Kille, W.E. Lees, B.M. Darke, D.R. Winge, C.T. Dameron, P.E. Stephens, and J. Kay, J. Biol. Chem., 267 (1992) 8042–8049.
[258] T. Oikawa, N. Esaki, H. Tanaka, and K. Soda, Proc. Natl. Acad. Sci. USA, 88 (1991) 3057–3059.
[259] J.R. Casas-Finet, S. Hu, D. Hamer, and R.L. Karpel, FEBS Letters, 281 (1991) 205–208.
[260] S.S. Hasnain, G.P. Diakun, I. Abrahams, I. Ross, C.D. Garner, I. Bremner, and M. Vasak, in J.H.R. Kagi, and Y. Kojima, eds. Metallothionein II, Birkhauser Verlag, Basel 1987, pp 227–236.
[261] I.L. Abrahams, and C.D. Garner, J. Am. Chem. Soc., 107 (1985) 4596–4597.
[262] H. Rupp, and U. Weser, FEBS Letters, 44 (1974) 293–297.
[263] C.D. Garner, S.S. Hasnain, I. Bremner, and J. Bordas, J. Inorg. Biochem., 16 (1982) 253–256.
[264] R.W. Briggs, and I.M. Armitage, J. Biol. Chem., 257 (1982) 1259–1262.